FGF8-mediated signaling regulates tooth developmental pace and size during odontogenesis

Chensheng Lin[1], Ningsheng Ruan[1], Linjun Li[1], Yibin Chen[1], Xiaoxiao Hu[1], YiPing Chen[2], Xuefeng Hu[1]*, Yanding Zhang[1]*

[1]Fujian Key Laboratory of Developmental and Neural Biology & Southern Center for Biomedical Research, College of Life Sciences, Fujian Normal University, Fuzhou, Fujian, 350117, P.R. China.

[2]Department of Cell and Molecular Biology, Tulane University, New Orleans, LA 70118, USA.

Running title: FGF8 regulates tooth developmental pace and size

***Correspondence to:**

Yanding Zhang, Ph.D.

College of Life Sciences, Fujian Normal University (Qishan Campus), Fuzhou, Fujian, 350117, P.R. China.

Phone: +86-13706963408 (tel); E-mail: ydzhang@fjnu.edu.cn

or

Xuefeng Hu, Ph.D.

College of Life Sciences, Fujian Normal University (Qishan Campus), Fuzhou, Fujian, 350117, P.R. China.

Phone: +86-13055734898 (tel) ; E-mail: bioxfh@fjnu.edu.cn

This manuscript is available as a preprint on non-commercial server bioRxiv: https://doi.org/10.1101/2020.09.16.299388.

Disclosure page

Conflicts of interest

The authors declare no conflicts of interest.

Data Availability Statement

All the data are available within the article or its supplementary materials.

Abstract

The developing human and mouse teeth constitute an ideal model system to study the regulatory mechanism underlying organ growth control due to the fact that their teeth share highly conserved and well-characterized developmental processes and their developmental tempo and size vary notably. In the current study, we manipulated heterogenous recombination between human and mouse dental tissues and demonstrate that the dental mesenchyme dominates the tooth developmental tempo and size and FGF8 could be a critical player during this developmental process. Forced activation of FGF8 signaling in the dental mesenchyme of mice promoted cell proliferation, prevented cell apoptosis via p38 and perhaps PI3K-Akt intracellular signaling, and impelled the transition of the cell cycle from G1- to S-phase in the tooth germ, resulting in the slowdown of the tooth developmental pace and the enlargement of the tooth size. Our results provide compelling evidence that extrinsic signals can profoundly affect tooth developmental tempo and size and the dental mesenchymal FGF8 could be a pivotal factor in controlling developmental pace and size in a non-cell-autonomous manner during mammalian odontogenesis.

Key words: FGF8, tooth, developmental pace, size, non-cell-autonomous.

52 # Introduction

53 Although mammals possess an almost identical body plan with morphologically and
54 functionally similar organs and systems, their developmental tempo and body sizes vary
55 greatly among different species. Generally, larger-bodied species own longer gestation
56 lengths with slower developmental tempos to acquire larger body sizes (Promislow and
57 Harvey, 1990, Swanson and Dantzer, 2014). Obviously, developmental tempo and organ
58 size must be tightly harmonized to ensure the correct establishment of body plan and
59 therefore both of them are the result of a precisely controlled process. The mechanisms
60 that regulate organ growth (i.e. embryonic development and postnatal growth) and size
61 have been well investigated in non-mammalian models, particularly in *Drosophila*
62 *melanogaster*, in which roles of TOR (target of rapamycin), insulin/IGF (insulin-like
63 growth factor), Ras/Raf/MAPK, JNK (c-Jun N-terminal kinase), and Hippo signaling
64 pathways are well defined (Gokhale and Shingleton, 2015).

65 In mammals, several conserved families of secreted growth factors, including FGF
66 (fibroblast growth factor), BMP (bone morphogenetic protein), TGF-β (transforming
67 growth factor-β), GH (growth hormone)/IGF, and Hippo/YAP, are deemed to be involved
68 in the regulation of organ growth and organ size due to their ability to modulate cell
69 proliferation and apoptosis during embryonic development (Penzo-Mendez and Stanger,
70 2015, Lui et al., 2015, Gokhale and Shingleton, 2015). However, no direct evidence can
71 explain roles of pathways abovementioned in controlling developmental pace and organ
72 size in mammals, except for the Hippo and IGF pathway in size control (Barry et al., 2013,
73 Liu et al., 2014, Yu et al., 2015, Zhang et al., 2017, Tumaneng et al., 2012, Zaina and
74 Squire, 1998).

75 Mammalian teeth have long served as a model organ for studying fundamental
76 questions in organ development on the molecular basis (Zhang et al., 2005). The main
77 features of tooth morphogenesis are conserved in the mammalian lineage (Polly, 2015,
78 Jheon et al., 2013, Salazar-Ciudad, 2012), as they are all formed by sequential and
79 reciprocal interactions between epithelium and mesenchyme and share similar processes
80 during tooth development (Jheon et al., 2013). Despite these considerable homologies,

mammalian dentition undergoes remarkable morphological diversification, displaying great variations not only in tooth shape and number but also tooth size and growth rate (Schoenwolf GC, 2014, Rodrigues et al., 2013, Jheon et al., 2013, Zhang et al., 2005, Line, 2003). Obviously, the human dentition appears much larger size than the mouse one. In addition, the period of tooth development in humans takes about 400 days from the initiation stage at embryonic 6th week to tooth eruption at postnatal 6th month. Whereas, this period in mice takes only about 20 days from the determination of tooth forming sites at E10.5 to tooth eruption at postnatal 10th day (Zhang et al., 2005). Thus, the human and mouse embryonic tooth provides an ideal model system for investigating the regulatory mechanism underlying the developmental tempo and size.

It is generally believed that diversified forms of organ morphogenesis (including growth rate and size) among species are achieved by tinkering conserved signaling pathways instead of proposing novel ones during development (Edelman, 1992, Thesleff and Sharpe, 1997, Jernvall and Thesleff, 2000). The difference in organismal growth rate and organ or body size between humans and mice primarily reflect the difference in cell number rather than the cell size (Lloyd, 2013). Many lines of evidence from mouse models demonstrate that numerous growth factors of conserved families, such as FGF, BMP, SHH, and Wnt, have been shown to play critical roles in tooth morphogenesis by regulating cell proliferation, differentiation, and apoptosis during odontogenesis (Tummers and Thesleff, 2009, Plikus et al., 2005, Tapaltsyan et al., 2016, Jheon et al., 2013, Thesleff and Sharpe, 1997, Thesleff and Mikkola, 2002, Tucker and Sharpe, 2004, Salazar-Ciudad, 2012). Studies in mice demonstrated that the Hippo pathway, a signaling pathway that is well-known to control organ size in mammals, does not involve in the regulation of tooth developmental pace and size during odontogenesis (Liu et al., 2014, Kwon et al., 2015) , but tuning down the BMP signaling by overexpressing secreted *Noggin* in the dental epithelium could reduce the tooth size. Here, we took advantage of the differences in developmental tempo and size of teeth in mice and humans, and provide compelling evidence that it is the dental mesenchyme that dominates tooth developmental tempo and size in a non-cell-autonomous manner and extrinsic FGF8 may act as a critical factor in controlling these processes during odontogenesis.

111 # Materials and methods

112 **Mouse models**

113 *Wnt1-Cre* and *R26R*^{Fgf8} mice were described previously (Danielian et al., 1998, Lin et al., 2013).
114 Dental mesenchyme-specifically overexpressed *Fgf8* mice were generated by crossing
115 *Wnt1-Cre* mice with *R26R*^{Fgf8} mice. Mutant embryos were identified by PCR genotyping.
116 All wild-type mice were on the CD-1 background. Mice were housed under the following
117 identical conditions: 40-70% relative humidity, 12 hour light/dark cycle, and 20-25°C
118 ambient temperature, in individually ventilated cages, with corncob granules for bedding
119 and nesting, in groups of up to six. The mice were given free access to tap water and
120 standard rodent chow (1010011; Jiangsu Xietong Pharmaceutical Bio-engineering Co.,
121 Ltd, Nanjing, China).

122 **Tissue recombination, organ culture, and subrenal culture**

123 Fresh lower jaws isolated from human fetuses of 14th-16th week gestation following
124 medical termination of pregnancy were provided by Maternal and Child Health Hospital
125 of Fujian Province, China. The precise embryonic age of fetuses was defined by the
126 measurement of the crown-rump length (CRL) (Hu et al., 2014a). Human and E13.5
127 mouse embryonic tooth germs were dissected out in ice-cold PBS and then treated with
128 Dispase II at 37℃ for 20 min. The dental mesenchyme and dental epithelium were
129 separated with the aid of fine forceps and incubated on ice for further tissue recombination
130 experiments. Three types of tissue recombination were conducted and are summarized in
131 Table 1: E13.5 mouse dental epithelium with bell-stage human dental mesenchyme (14-
132 16 weeks of gestation) (referred to as mde+hdm); E13.5 mouse dental mesenchyme with
133 bell-stage human dental epithelium (hde+mdm); and E13.5 mouse dental mesenchyme
134 with mouse dental epithelium from the same stage as control (mde+mdm). All
135 recombinants were cultured in the Trowell-type organ culture dish overnight, followed by
136 subrenal grafting in adult nude mice, as described previously (Zhang et al., 2003, Hu et
137 al., 2014a). The use of animals and human tissues in this study was approved by the Ethics
138 Committee of Fujian Normal University (permission #2011005).

139 **SU5402 injection**

140 Two first mandibular premolar germs dissected out from the lower jaw of a human
141 fetus of 16th week gestation were cultured under the kidney capsules of two nude mice,
142 one germ each. SU5402 (Calbiochem, California, USA) and DMSO (Merck, Darmstadt,
143 Germany) was intraperitoneally injected into each recipient mouse at a dose of
144 25mg/Kg/d in 200 μL PBS twice a day for one week. The human tooth grafts were
145 harvested for histological analysis after another week in subrenal culture.

146 **Lentivirus infection and cell re-aggregation**

147 For efficient infection of lentivirus (Song et al., 2006), isolated E13.5 mouse dental
148 mesenchyme was digested with 0.25% trypsin at 37 °C for 5 min and dispersed into a
149 single-cell suspension with the aid of a micropipette. To make a dental mesenchyme pellet,
150 about 5×10^5 dental mesenchymal cells were infected with 20 μL concentrated lentivirus
151 in 200 μL culture medium in an Eppendorf tube. The tube was incubated at 37℃ in a 5%
152 CO_2 environment for 2 hours with its cap open, centrifuged at 3000 rpm for 3 min, and
153 then incubated again in the same environment for 2 hours. Cell pellets were removed from
154 the tubes, recombined with E13.5 dental epithelium, and cultured in the Trowell-type
155 organ culture dish overnight. Recombinants were subsequently subjected to subrenal
156 culture in nude mice.

157 **Histology, *in situ* hybridization, immunostaining, and Western blot**

158 For histological analysis, harvested samples were fixed in 4% paraformaldehyde
159 (PFA)/PBS, dehydrated, embedded in paraffin, and sectioned at 7 μm. Standard
160 Hematoxylin/Eosin (H&E) and Azan dichromic staining were utilized for histological
161 analysis (Hu et al., 2014b). Ossified tissues or grafts were demineralized with EDTA/PBS
162 for a week prior to dehydration. For *in situ* hybridization, dental tissues from staged
163 human embryos were dissected out in ice-cold PBS and fixed in 4% RNase-free PFA/PBS
164 at 4°C overnight. Human cDNAs, including *FGF1* (MHS6278-202758608), *FGF2*
165 (EHS1001-208062206), *FGF15/19* (MHS6278-202756089), *FGF18* (MHS6278-
166 202830446), were purchased from Open Biosystems (Alabama, USA) and were
167 subcloned to pBluescript-KS plus vector for riboprobe transcription. Whole-mount *in situ*
168 hybridization and section *in situ* hybridization were performed following standard
169 protocols as described previously (St Amand et al., 2000, Dong et al., 2014).

170 Immunostaining was performed as described previously (Xiong et al., 2009). The
171 following primary antibodies were used including the products of Santa Cruz
172 Biotechnology (Texas, USA): Ameloblastin, MMP20, DSP, K-Ras, FGF8, P21; ABCam:
173 FGF4, FGF9, Caspase3, Ccnd1; Cell Signaling Tech (Massachusetts, USA): pSmad1/5/8,
174 pP38, pErk1/2, pJNK, pAKT1; Merck Millipore: β-catenin; and Spring Bio: Ki67. Alexa
175 Fluor 488 or 594 IgG (H+L) antibody (Thermo Fisher, Massachusetts, USA) and
176 horseradish peroxidase-coupled IgG antibody (Santa Cruz) were used as the secondary
177 antibody. For immunoblotting, pP38, pErk1/2, pJNK, pAkt, and Actin (Santa Cruz) were
178 used as primary antibodies. IRDye 800cw or 680cw IgG (Odyssey, Nebraska, USA) were
179 used as secondary antibodies. Immunoblotting was conducted as described previously
180 (Yang et al., 2014). Signals were observed using microscope (Olympus BX51, Tokyo,
181 Japan), Laser scanning confocal microscope (Zeiss LSM780, Jena, Germany), and
182 Infrared Imaging Systems (Odyssey Clx). Representative images were taken from a
183 minimum of 3 replicate experiments.

184 **Micro-computed tomography imaging and analysis**

185 Harvested mineralized teeth were scanned with X-ray micro-computed tomography
186 (microCT) equipment (μCT50, SCANCO Medical AG, Bruettisellen, Switzerland). The
187 microCT parameters were as follows: 19 × 19 mm-field of view, 15-μm voxel size, 70
188 kVp, 200 mA, 360° rotation, 1500ms exposure time. All datasets were exported in the
189 DICOM format with the isotropic 15-μm^3 voxel. Acquired height and width of the tooth
190 crown were analyzed with the attached software of μCT50.

191 **Statistics analysis**

192 Image J software (version 1.46r; National Institutes of Health, USA) was utilized for
193 Ki67-positive cell counting and to detect the densitometry of the western blot bands with
194 at least three biological replicates counted. Statistical analyses were performed with
195 GraphPad Prism 5 (Version 5.01; GraphPad Software Inc, California, USA). Data were
196 represented as mean ± SD. Paired *t*-test was used to evaluate differences between two
197 groups, and analysis of variance (ANOVA) was used to determine differences among
198 different groups. If there was a significance of ANOVA test, Bonferroni post-tests was
199 used. p values <0.05 is considered statistically significant difference.

Results

Tooth developmental tempo and size is dominated by the dental mesenchyme in humans and mice.

Our previous studies have showed that epithelial sheets of human keratinocyte stem cells, when recombined with E13.5 mouse dental mesenchyme, can be induced to differentiate into enamel-secreting ameloblasts in only 10 days and apoptotically degraded in 4 weeks to achieve small-sized chimeric teeth with similar size to mouse ones, whereas the mouse secondary branchial arch epithelium, when recombined with the human dental mesenchyme from the bell-stage, remains in an enamel-secreting status after 15-week *ex vivo* culture and acquired large-sized teeth in the end, a size similar to human deciduous teeth (Hu et al., 2014a, Wang et al., 2010, Hu et al., 2018). These results strongly imply that the duration of epithelial differentiation and size control in tooth development could be dominated by the mesenchymal component in humans and mice. To validate our hypothesis, we comprehensively revisited these phenotypes by carrying out meticulously designed heterogenous recombination between human and mouse embryonic dental tissues (Table 1). As shown in Fig. 1A-C, it took more than 4 weeks for the mouse dental epithelium to deposit enamel when recombined with the human dental mesenchyme in mde+hdm chimeric tooth germs, exhibiting a much longer developmental duration and slower tempo in comparison with the mouse dental epithelia that were combined with their own dental mesenchyme (Fig. 1E-G). By contrast, it took only about 10 days for the human dental epithelium to deposit enamel when recombined with E13.5 mouse dental mesenchyme in hde+mdm chimeric tooth germs (Fig. 1I-K), demonstrating a dramatically accelerated developmental pace compared to the normal human tooth morphogenesis. When the mouse dental epithelia were recombined with the human dental mesenchyme, in addition to the compliance of developmental pace with that of the human dental mesenchyme, the chimeric tooth germ generated an enlarged tooth after 16-week growth for sufficient mineralization (Fig. 1D), whereas when the human dental epithelium was recombined with the mouse dental mesenchyme, the developmental pace of chimeric teeth did not obeys that of the human dental epithelium but that of the mouse dental

229 mesenchyme, and thereby achieved a compact-size tooth equivalent to the size of mouse
230 homogenous (mde+mdm) teeth after grown under the kidney capsule for 30 days (Fig.
231 1H,L). Immunostaining of two ameloblastic differentiation markers, ameloblastin and
232 MMP20 (Matrix Metallopeptidase 20), further confirmed the development phase
233 alteration of the dental epithelium induced by the heterogenous dental mesenchyme. The
234 expression of these two markers in the mouse dental epithelium-derived pre-ameloblasts
235 in mde+hdm chimeric recombinants was delayed to 4th week in subrenal culture (Fig.
236 1M-O), whereas the expression of the two markers was antedated at 9-day in the human
237 dental epithelium-derived ameloblasts in hde+mdm chimeric recombinants in subrenal
238 culture (Fig. 1S-U), which is similar to the expression of them at 7-day in the ameloblasts
239 derived from the mouse dental epithelium in mde+mdm control recombinants (Fig. 1P-
240 R). The possibility of tissue contamination was ruled out using specific primary
241 antibodies against mouse or human MHC I antigens to distinguish between human and
242 mouse tissues in the heterogenous chimeras (Fig. S1). Our results unambiguously indicate
243 that the dental mesenchyme is a crucial component that dominates the tooth
244 developmental pace and size by interaction with the dental epithelium via diffusible
245 paracrine signals during odontogenesis.

246 **FGF signaling participates in the regulation of tooth developmental pace and size.**

247 We next attempted to identify the paracrine signaling molecules that may be
248 involved in the regulation of tooth developmental tempo in humans and mice. Despite the
249 fact that Hippo pathway that is present during tooth development as well is currently the
250 only well-recognized signaling pathway in the control of the size and growth rate for
251 several organs such as liver, knockout or overexpression experiments do not demonstrate
252 its function in the supervision of developmental pace and size during tooth development
253 (Liu et al., 2014, Kwon et al., 2015). Conserved SHH, FGF, BMP, and Wnt pathways are
254 all crucial signaling engaged in cell proliferation, apoptosis and differentiation during
255 odontogenesis, indicating that they may be key players in orchestrating the fundamental
256 mainspring of organ growth. Since the dental mesenchyme is dominant in the regulation
257 of tooth growth (Fig. 1), we exclude epithelially expressed SHH (Hu et al., 2013). To test

258 whether mesenchymal BMP, FGF and WNT signaling may be involved in the regulation
259 of tooth developmental pace and size, we examined the level of the active indicators of
260 these pathway including pSmad1/5/8 for BMP, K-Ras for FGF, and β-catenin for Wnt,
261 respectively, in the chimeric tooth germs. The expression level of K-Ras in both the dental
262 epithelium and mesenchyme is much higher in the mde+hdm chimeric tooth germ (Fig.
263 2E), where the development of mouse dental epithelium-derived ameloblasts were
264 dramatically delayed and remained immature after 4 weeks in subrenal culture, compared
265 to that in the mouse homogenous recombinant tooth germ (Fig. 2B). By contrast, the
266 expression levels of pSmad1/5/8 and β-catenin did not display obvious difference as
267 compared between the heterogenous recombinants and homogenous ones (Fig.
268 2A,C,D,F). The enhanced epithelial FGF activity in the mde+hdm chimeric tooth germ,
269 evidenced by outstandingly enhanced activity of K-Ras, was certainly induced by the
270 human dental mesenchyme and may attribute to the protracted differentiation of the
271 mouse dental epithelium.

272 To explore whether the upregulated FGF signaling may be associated with the
273 prolonged tooth development phase and large tooth size in humans, we started with a
274 search for candidate FGFs that are persistently expressed in the human developing dental
275 mesenchyme but barely in the mouse one. Most expression patterns of 22 known FGF
276 ligands in mammals have been verified in mouse tooth germs at the cap and bell stages
277 (summarized in Table S1)(Li et al., 2014, Cam et al., 1992). We have examined in our
278 previous studies the expression patterns of *FGF3, FGF4, FGF7, FGF8, FGF9,* and
279 *FGF10* in human tooth germs at different stages using *in situ* hybridization or
280 immunohistochemistry (Huang et al., 2015). Here, we screened the expression of
281 additional 12 *FGFs* that have not been identified in human tooth germs by RT-PCR. We
282 excluded *FGF11, FGF12, FGF13,* and *FGF14*, because they are not secreting ligands
283 and do not activate FGF receptors as well. We found that, among them, the transcripts of
284 *FGF1*, *FGF2*, *FGF15/19*, and *FGF18* were detectable at both the cap and bell stages
285 (data not shown). We further confirmed their expression in developing human teeth by
286 section *in situ* hybridization (Fig. S2). Comparison of FGF expression data between the
287 human (Huang et al., 2015) and mouse (Li et al., 2014, Cam et al., 1992), we noticed that

288 the majority of FGF transcripts are broadly distributed in the whole tooth germ including
289 the dental epithelium and mesenchyme throughout the early cap stage to the late bell stage
290 in humans (Huang et al., 2015). However, their expression is restricted to the limited
291 region of tooth germs, such as enamel knot, and appeared in limited periods of time in
292 mice (Table S1)(Li et al., 2014, Cam et al., 1992). We believe that this widely and
293 persistently distributing pattern of FGF ligands in the human tooth germs is closely related
294 to their characteristics of tooth development. To further verify this notion, we cultured
295 human 1st premolar germs at the early bell stage under the kidney capsule of nude mice
296 with intraperitoneal injection of SU5402, a global FGF-signaling inhibitor, for one week
297 and found accelerated detinogenesis in the SU5402-treated molar germ with the
298 appearance of both predentin and dentin (Fig. 2G), as compared to DMSO-treated one
299 with appearance of only predentin (Fig. 2H), indicating pivotal roles of FGF-signaling in
300 regulation of tooth developmental tempo.

301 With further analyses of FGF expression data in humans and mice, we found that
302 FGF4, FGF8, and FGF9 ligands exhibit most distinctive patterns (Table S1). These three
303 ligands are persistently expressed in the dental epithelium and mesenchyme at least until
304 the differentiation stage in humans (Huang et al., 2015). However, in mice, the expression
305 of FGF4 is restricted to the enamel knot from the cap to bell stage and that of FGF9 to
306 the enamel knot at the cap stage and to the dental epithelium at the bell stage. Furthermore,
307 FGF8 is only expressed in the presumptive dental epithelium prior to and during the
308 laminar stage and is no longer expressed after the E12 bud stage (Kettunen and Thesleff,
309 1998). Whereas, in humans, *FGF8* transcripts are widely and intensively present in the
310 whole tooth germ at least from the early cap stage to the differentiation stage (Huang et
311 al., 2015). Importantly, we found retained expression of FGF8, as well as FGF4 and FGF9,
312 in the mouse dental epithelium derived pre-ameloblasts in mde+hdm recombinants after
313 4 week in subrenal culture, where the development of mouse ameloblasts was largely
314 delayed (Fig. 2I-K). Based on these observations, we hypothesized that FGF signaling
315 may play important roles and FGF8 could be a critical factor in the regulation of tooth
316 developmental pace and size.
317

318 **Forced activation of FGF8 signaling in the mouse dental mesenchyme delays tooth**
319 **development and enlarges tooth size.**

320 To test our hypothesis, we set to overexpress *Fgf8* in dental mesenchymal cells in
321 the E13.5 recombinant molar germ via lentivirus-mediated expression and subrenal
322 culture system. Histological examination revealed that it took up to 9 days for *Fgf8*-
323 overexpressed tooth grafts to start dentin secreting (Fig. 3B), whereas it only took 7 days
324 for control ones to do so (Fig. 3A). Moreover, Ki67 staining detected remarkably higher
325 level of proliferation rate in both the dental epithelium and mesenchyme of *Fgf8*-
326 overexpressed tooth grafts compared to the controls after 7 days in subrenal culture (Fig.
327 3C-E; *n*=6/group). These data indicate that activated mesenchymal FGF8 activity delays
328 tooth development and dramatically stimulates cell proliferation.

329 To corroborate the aforementioned *ex vivo* results, we further generated *Wnt1-Cre;*
330 $R26R^{Fgf8}$ transgenic mice to verify whether forced activation of mesenchymal FGF8
331 signaling alters tooth development *in vivo*. The presence of FGF8 in the dental
332 mesenchyme of *Wnt1-Cre;*$R26R^{Fgf8}$ mice was confirmed by anti-FGF8 immunostaining
333 (Fig. S3). Most of mutant embryos die at around E12.5 and a few died around E14.5.
334 Although histological examination revealed severe craniofacial hypoplasia in 100% cases,
335 including exencephaly and the absence of identifiable tissues such as ears, auricles, eyes,
336 nose, as well as tongue (data not shown), the mutant mice still possessed a pair of intact
337 maxillary and mandibular molar germs (Fig. 4). More importantly, both the maxillary and
338 mandibular molar germ exhibited an obvious retardation of tooth development (Fig. 4).
339 Since most mutant embryos died at around E12.5, we grafted E11.5 mutant molar germs
340 under the kidney capsule for further development. Examination of histology and the
341 deposition of dentin and enamel showed the mutant teeth developed with approximate
342 one-day's delay when compared to the wild-type ones (Fig. 5A-F). Examination of the
343 expression of odontoblast marker DSP and ameloblast marker ameloblastin in the grafted
344 teeth further confirmed this delay (Fig. 5I-L).

345 Interestingly, Azan staining showed that the mutant graft formed a larger-sized tooth
346 (Fig. 5G) than the wild-type one (Fig. 5H) after 18 days in subrenal culture. To precisely
347 evaluate the effect of mesenchymal *Fgf8* on tooth size, the tooth grafts were cultured

348 under the kidney capsule for 3 months for complete mineralization. Micro-CT scanning
349 revealed that the mutant graft indeed formed a larger-sized tooth with short and dumpy
350 shape (Fig 5N) compared to the control (Fig. 5M). Measurement of the height and width
351 of the tooth crowns exhibited no difference in the average height of the tooth crowns
352 between the mutants (n = 11) and wild-types (n = 7) but about 20% wider in the average
353 width in the mutants compared to the controls (Fig. 5O). Apparently, higher rate of cell
354 proliferation contributes greatly to the larger teeth, which was evidenced by more Ki67
355 positive cells presented in E13.5 mutant tooth germ and the grafted mutant teeth than
356 controls (Fig. 6A-F, K-M, n = 3/each group). Meanwhile, while apoptotic marker
357 Caspase3 staining was present in ameloblasts and odontoblasts in both mutant (Fig. I,J)
358 and wild-type tooth germs (Fig. 6G,H), this apoptotic signal was non-detectable in the
359 pulp cells of mutant tooth germs (Fig. 6I,J), whereas it was seen in that of wild-type ones
360 (Fig. 6G,H) after 18 days in subrenal culture. These results further support the idea that
361 ectopically activated FGF8 signaling in the mouse dental mesenchyme stimulates cell
362 proliferation and prevents cell apoptosis during odontogenesis.

363 **Ectopically activated dental mesenchymal FGF8 signaling is transduced via p38 and**
364 **PI3K-Akt intracellular pathway.**

365 To determine which intracellular pathway is implicated in the signal transduction of
366 the ectopically activated dental mesenchymal FGF8 signals, we examined the levels of
367 phosphorylated Erk1/2, P38, JNK, and PI3K-Akt, the activity indicator of MAPK
368 pathway, in both E13.5 tooth germs and E11.5 ones after 9 days in subrenal culture. As
369 shown in Fig. 7, no signal intensity differences in pErk1/2 (Fig. 7A-D) and pJNK (Fig.
370 7E-H) staining were observed between wild-type and mutant teeth. Whereas, p38
371 signaling is dramatically elevated in *Wnt1-Cre;R26R*^{Fgf8} teeth with a considerably
372 increased amount of nuclear-localized pP38 cells both in the dental epithelium and dental
373 mesenchyme of E13.5 mutant tooth germs (Fig. 7J) and grafted teeth (Fig. 7L) as
374 compared to the controls (Fig. 7I,K). Meanwhile, the intensity of PI3K-Akt staining was
375 slightly enhanced and the amount of pAkt1^{+} cells was increased in mutant E13.5 tooth
376 germs and grafted teeth (Fig. 7N,P) as compared to controls (Fig7 M,O). Western blot

377 analysis further confirmed the increased expression of pP38 and pAkt1 in E13.5 mutant
378 tooth germs (Fig. 7Q,R; n = 3). Our results indicate that the augmented dental
379 mesenchymal FGF8 activity enhances P38 and PI3K-Akt signaling in both the dental
380 mesenchyme and the dental epithelium, suggesting that they may function as intracellular
381 pathways for transducing FGF8 signal into nuclei.

382 **Enhanced dental mesenchymal FGF8 signaling promotes transition of cell cycle**
383 **from G1- to S-stage during odontogenesis.**

384 The rate of cell proliferation controlled by cell cycle progression is a key player in
385 organ size control (Gokhale and Shingleton, 2015) and is also closely associated with
386 tissue differentiation status, as higher cell proliferation always presents in developing
387 tissues and lower one in differentiated ones. Since the elevation of *Fgf8* expression in the
388 dental mesenchyme results in the significant promotion of cell proliferation and
389 prevention of cell apoptosis (Fig. 6), we speculated that enhanced dental mesenchymal
390 FGF8 signaling would alter cell cycling. To verify this hypothesis, we set forth to
391 ascertain the distribution of cyclin D1 (Ccnd1) and its inhibitor $p21^{Cip1}$ (p21), a pair of
392 critical regulators functioning stimulatory and repression effect, respectively, on inducing
393 cell cycle entry and mediating the G1-S stage transition (Baldin et al., 1993, Gartel and
394 Radhakrishnan, 2005), in E13.5 tooth germs and grafted teeth. As shown in Fig. 8,
395 although the same high density of $Ccnd1^+$ cells were present in the dental epithelium of
396 E13.5 wild-type and mutant tooth germs, the dental mesenchyme in mutant tooth germs
397 possessed an considerably increased amount of $Ccnd1^+$ cells in comparison to that in
398 wild-type ones (Fig. 8A,E). On the other hand, $p21^+$ cells were abundantly present in the
399 presumptive primary enamel knot of the dental epithelium and slightly in the dental
400 mesenchyme in wild-type tooth germs but totally absent from the whole tooth germ in
401 mutant ones (Fig. 8B,F). Thereout, more nuclear colocalization of Ccnd1 and p21 staining
402 were found in the presumptive primary enamel knot of the wild-type tooth germs than in
403 the mutant ones (Fig. 8C-D, G-H), which makes p21 functioning with Ccnd1 to regulate
404 the cell cycle progression and inhibits cell proliferation in the epithelial signal center in
405 the wild-type tooth germ. In grafted teeth, nuclear $Ccnd1^+$ cells were distributed not only

406 in ameloblasts and odontoblasts (Fig. 8M,P-up) but also all over the dental pulp in
407 mutants (Fig. 8M,P-down), rather than being restricted to the dental mesenchymal cells
408 adjacent to the odontoblasts in wild-types (Fig. 8I,L). Although p21 was expressed in
409 ameloblasts and dental mesenchymal cells in both wild-type and mutant teeth, its
410 expression level was relatively decreased in mutants (Fig. 8J,L,N,P). In addition, the
411 nuclear localization of p21 could be detected in dental mesenchymal cells of wild-type
412 teeth (Fig. 8L-down), whereas it was found to be in the cytoplasm of grafted mutant teeth
413 (Fig. 8P-down), which make it unable to cooperate with nuclear Ccnd1 to regulate the
414 cell cycle progression in the dental mesenchymal cells. Taken together, these results
415 provide evidence that enhanced mesenchymal FGF8 activity observably elevates the
416 activity of nuclear Ccnd1 while degrades the activity of nuclear p21. Thus both
417 stimulation of Ccnd1 and repression of p21 function to induce cell cycle entry and
418 promote the transition of cell cycle from G1- to S- stage, which facilitates cell population
419 to retain the high rate of proliferation.

420 # Discussion

421 Hippo signaling is the only admitted pathway that plays its best-known physiological
422 function on the control of organ size in the mouse model for mammalian lineage (Barry
423 et al., 2013, Liu et al., 2014, Yu et al., 2015, Zhang et al., 2017), which mainly involves
424 in the regulation of cell proliferation and apoptosis and thereby cell number (Tumaneng
425 et al., 2012). Activation or inhibition of YAP/TAZ, a transcriptional co-activator of Hippo
426 pathway, leads to the adjustment of cell proliferation and apoptosis, thus affecting organ
427 sizes and tissue homeostasis (Barry et al., 2013, Liu et al., 2014, Yu et al., 2015, Zhang et
428 al., 2017). However, in tooth development, suppression of YAP *ex vivo* at the cap stage
429 only leads to ectopic cusp formation (Kwon et al., 2015), while overexpression of YAP
430 *in vivo* disrupts tooth morphogenesis with abnormal enamel knot as well as greatly
431 widened dental lamina; teeth ultimately formed in YAP transgenic mice do not exhibit
432 any growth delay or size enlargement (Liu et al., 2014). These data suggest that the
433 renowned control function of Hippo pathway in mammalian organ size is not applicable
434 for the tooth organ. In support of this notion, it has also been reported that size-control
435 mechanisms differ across mammalian organs (Penzo-Mendez and Stanger, 2015) and
436 enhanced Hippo signaling induces organ enlargements in the stomach, heart, liver, and
437 spleen, but not in lung, kidney, and intestine (Song et al., 2010, Heallen et al., 2011, Dong
438 et al., 2007). Besides, IGF signaling is the other pathway that has been implied to have
439 effects on organ size since *Igf2r* disrupted mice are born 25-35% bigger than wild-types,
440 however, it has also been revealed that IGF signaling affects the size in some organs such
441 as the cecum and colon but not the size of other organs such as the skin and stomach
442 (Zaina and Squire, 1998), which also support the notion.

443 A heterogenous recombination study carried out between the mouse and rat molar
444 tooth germs has suggested that tooth size is determined by the dental mesenchyme (Cai
445 et al., 2007, Jiang et al., 1999). Additionally, our recent studies showed that, in
446 comparison with natural developmental pace, the differentiation duration of the mouse
447 dental epithelium or non-dental epithelium into ameloblasts when induced by the human
448 dental mesenchyme is significantly extended, whereas that of the human dental

epithelium or epithelial stem cells into ameloblasts when induced by the mouse dental mesenchyme is significantly shortened (Wang et al., 2010, Hu et al., 2018). These results are consistent with the difference of development progression speed between human and mouse teeth (Zhang et al., 2005), suggesting a dominant role of the dental mesenchyme in regulation of tooth developmental tempo. This idea is further supported by our current heterogenous recombination study carried out between the mouse and human molar tooth germs (Fig. 1). We further provide unambiguous evidence that not only the tooth size but also the tooth developmental pace are obedient to hereditary character of the dental mesenchyme.

Conserved pathways, such as FGF, BMP, Hh, and WNT pathway, participate in the highly conserved molecular mechanism underlying organismal growth by corresponding alterations of cell growth and division (Penzo-Mendez and Stanger, 2015, Lui et al., 2015, Gokhale and Shingleton, 2015). FGFs, as the most common mitogens, are positively correlated to the rate of cell growth and cell division and involved in the induction and pattern formation during tooth development (Brewer et al., 2016, Lan et al., 2014). Fgf8 has been demonstrated to play an important role in cell survival and proliferation of CNC cells (Abzhanov et al., 2003), and to exert a positive effect on proliferation of dental mesenchymal cells (Kettunen and Thesleff, 1998). Our data show that FGF signaling rather than BMP and WNT signaling is highly active in human-mouse chimeric tooth germs where the differentiation duration of the mouse dental epithelium is largely slowed down (Fig. 2), which is consistent with the continuously high expression of FGFs, particularly FGF8, in human tooth germs, suggesting a potentially positive role of FGF signaling in regulating the tooth developmental tempo and size during odontogenesis in humans. Both our *ex vivo* lentivirus-mediated overexpression system and *in vivo* transgenic mouse model support that forcibly activated dental mesenchymal FGF8 signaling stimulates cell proliferation and inhibits cell apoptosis, thus prolonging tooth developmental pace and enlarges tooth size in mice (Fig. 3-6). FGF8 appears to be a critical factor in regulating the tooth developmental pace and size during mammalian odontogenesis.

Functional redundancy complicates interpretation of FGF genetic studies.

479 Phenotypes in various *Fgfr* knockout mice have demonstrated that different FGF
480 receptors have both essential and redundant roles throughout development (Brewer et al.,
481 2016). During odontogenesis, FGF7 and FGF10 have been proven to act as surrogates of
482 mesenchymal FGF3 (Kratochwil et al., 2002), and FGF4, FGF8, as well as FGF9 have
483 also been suggested functional redundancy and repetitive use in mouse tooth development
484 (Zhang et al., 2005). Our previous and current study show that several FGFs, especially
485 FGF4, FGF8, and FGF9, have a broad and persistent expression in the whole tooth germs
486 in humans but are restricted to the limited region of tooth germs in mice (Huang et al.,
487 2015) (Table S1). These data suggest that tooth developmental pace and size may be the
488 product of synergistic effects of different FGFs in mammals. Actually, in addition to the
489 fact that FGF8 is a key factor to control tooth developmental pace and size discovered in
490 the current study, Fgf9 has also been reported to induce cell proliferation in cultured
491 mouse dental mesenchyme *in vitro* (Kettunen and Thesleff, 1998) as well as in cervical
492 loop development *in vivo* (Kurosaka et al., 2011) and the *Fgf9* null mutant mice show a
493 size-reduced labial cervical loop (Kurosaka et al., 2011), and FGF4 stimulates cell
494 proliferation in both the dental epithelium and mesenchyme as well (Kettunen and
495 Thesleff, 1998, Jernvall et al., 1994), both suggesting their positive function on the
496 regulation of tooth growth and size. We speculate that, in humans, several broadly,
497 intensively, and persistently expressed FGF ligands may act in concert to confer growth
498 capability (stimulation of proliferation and prevention of apoptosis) on tooth tissues to
499 achieve longer development time-scale and larger size.

500 Transduction of FGF signaling is mediated by multiple intracellular pathways,
501 including P38, PI3K/Akt, Erk1/2, and JNK (Brewer et al., 2016). In our previous study,
502 the similar expression patterns of the indicators in Erk, P38, JNK, and PI3K-Akt pathways
503 in mouse and human tooth germs suggests their conservative regulatory functions during
504 mammalian odontogenesis (Huang et al., 2015). P38 has been reported to be involved in
505 control of the cell cycle via the expression changes of P21, P27 and Ccnd3 in mouse
506 skeletal muscle cells (Irazoqui et al., 2014), Ccnd1 and c-Myc in human dental pulp stem
507 cells (Vandomme et al., 2014), and Ccnd1 and P21 in rat mesenchymal stem cells (Stockl
508 et al., 2013), which is also significantly increased in our *Wnt1-Cre; R26R*^{Fgf8} mice (Fig.

509 7). The PI3K-Akt pathway is associated with a variety of cellular functions including cell
510 growth, cell cycle regulation, and cell survival (Castellano and Downward, 2011). The
511 increased PI3K-Akt level regulates the proliferation and differentiation of neural
512 progenitor cells by the activation of the cell cycle through the elevation of the Ccnd1 and
513 cyclin E, two cyclins essential for the G1-S transition during organogenesis (Xue and
514 Yuan, 2010). Moreover, Akt protein is a central intracellular factor to transduce and
515 integrate multiple extracellular growth factor signals, such as FGF, BMP, and GH/IGF,
516 into a comprehensive signal network to supervise the processes of cell proliferation,
517 growth, and survival (Penzo-Mendez and Stanger, 2015). The increased activity of PI3K-
518 Akt pathway caused by augmented FGF8 in the cranial neural crest cell (Fig. 7) further
519 supports its positive function in cell proliferation regulated by cell cycle during tooth
520 development. Erk has been reported to provide a switch-like transition between
521 proliferation and differentiation of muscle progenitors (Michailovici et al., 2014), while
522 JNK pathway has been elucidated to play crucial role in negative growth regulation and
523 likely performs a central regulator in both local growth coordination and global growth
524 coordination (Gokhale and Shingleton, 2015). These two pathways did not show any
525 noticeable alteration in our *Fgf8* transgenic mice, which may attribute to their main
526 function in control of negative growth or balancing cell proliferation and differentiation.
527 Cell growth and division are controlled by the cyclin depend kinases (CDKs) and
528 their binding partners (cyclins) that regulate cell cycle progression through the regulation
529 of the G1-S and G2-M transition. Many cell cycle regulators have been proved to control
530 organ growth and size, which appears to be generally conserved in *Drosophila* and
531 mammals (Gokhale and Shingleton, 2015). The G1-S phase transition is a rate-limiting
532 step, a known checkpoint between cell growth and cell division, requiring cell cycle
533 regulators to monitor and regulate the progression of the cell cycle (Elledge, 1996). The
534 stimulatory effects of cyclins can be offset by CDKs inhibitors (CDKIs) and the
535 repression of CDKIs is also a prerequisite for G1-S transition. Thus merely elevating the
536 level of cyclin D1 is not sufficient to induce cell cycle entry (Chambard et al., 2007).
537 Cyclin D1 (Ccnd1) is synthesized rapidly in the G1 phase and accumulates in the nucleus
538 and degraded as the cell enters the S phase (Baldin et al., 1993). P21, known as CDKI1,

539 functions as a regulator of cell cycle progression in G1 and S phase and inhibits all
540 cyclin/CDK complexes, which in turn results in cell cycle arrest and/or apoptosis (Gartel
541 and Radhakrishnan, 2005). Enhanced dental mesenchymal FGF8 may promotes cell cycle
542 progression through the regulation of the G1-S transition, which further stimulates cell
543 proliferation and prevents cell differentiation and apoptosis, thereby resulting in
544 prolonged tooth development and larger tooth size. In line with this notion, we found that
545 the amount of nuclear Ccnd1^{+} cells is dramatically increased while that of nuclear P21^{+}
546 cells is markedly decreased in the dental mesenchyme at both the early and differentiation
547 stage in *Wnt1-Cre;R26R*^{Fgf8} mice as compared to those in the control (Fig. 8), stating that
548 forcedly enhanced FGF8 in the dental mesenchyme could elevate the level of Ccnd1 and
549 meanwhile suppress the level of p21. Stimulation of Ccnd1 and repression of p21 both
550 constitute the prerequisite for inducing cell cycle entry and thereby promoting the G1-S
551 transition.

552 Two latest studies have demonstrated that interspecies differences in developmental
553 tempo are caused by cell-autonomous differences in biochemical reaction speeds instead
554 of differences in signaling, the sequence of genes, or regulatory elements in *in vitro*
555 human and mouse platforms (Rayon et al., 2020, Matsuda et al., 2020). Moreover, in
556 *Drosophila*, it is also reported that the *Minute* mutation causes a prolongation of
557 developmental pace and decreased cell division rate in a cell-autonomous way via
558 decreasing the expression of ribosomal proteins and thereby reducing the rate of
559 translation and protein synthesis (Saebøe-Larssen et al., 1998, Morata and Ripoll, 1975).
560 Developmental allochrony regulated in a cell-autonomous manner is highlighted in these
561 studies. However, our findings that the dental mesenchyme resorts to extrinsic signals
562 such as FGF to dominate the developmental tempo and size as well via tissue interaction
563 in a non-cell-autonomous manner during tooth development are inconsistent with these
564 studies. Additionally, the fact that the oscillation phase shift between Notch and Wnt
565 signaling is critical for the segmentation of presomitic mesoderm cells in multicellular
566 organ development in 2D assays *ex vivo* (Sonnen et al., 2018) also indicates the pivotal
567 role of secretory signal changes in the regulation of developmental pace. In *Drosophila*,
568 organ growth and size are orchestrated not only by the growth rate regulated via signaling

569 pathways but also by the growth duration regulated via hormonal signals and organ-
570 autonomous processes controlled by patterning genes and physical force (Gokhale and
571 Shingleton, 2015). The developmental tempo and size of individual organs must be tightly
572 coordinated to match the body size and larger-bodied species always keep slower
573 developmental tempos to acquire larger organ sizes. Our heterogenous recombination
574 results provide compelling evidence to support the contribution of extrinsic cues in the
575 developmental tempo and size of teeth relying on tissue interaction during early
576 development. Thus, we suggest that complicated regulatory networks involved in the
577 developmental pace and size work both in a cell-autonomous and non-cell-autonomous
578 way to orchestrate the organ morphogenesis, and, particularly, tissue interaction in a non-
579 cell-autonomous way plays a major role during early organogenesis.

580 Tissue bioengineering based on the principle of developmental biology represents a
581 promising approach for repair and regeneration of damaged tissues and organs in the
582 future. However, unmatched development phase and organ size between humans and the
583 model animals such as *Drosophila*, zebra fishes, and mice appear to be a major obstacle
584 to acquire knowledge about organ growth control in humans. Uncovering of the molecular
585 mechanism underlying organ growth control in humans is a prerequisite for the realization
586 of replacement therapy in the future. Our study provides important FGF signaling
587 information in tooth developmental process and enlightens our knowledge about the
588 nature of FGF signaling in human tooth growth.

Acknowledgments

This study was supported by the National Natural Science Foundation of China (81870739, 82001002, 81271102, 81771034) and the Natural Science Foundation of Fujian Province (2019J01281, 2020J01180).

References

Abzhanov, A., Tzahor, E., Lassar, A. B. & Tabin, C. J. 2003. Dissimilar regulation of cell differentiation in mesencephalic (cranial) and sacral (trunk) neural crest cells in vitro. *Development,* 130**,** 4567-79.

Baldin, V., Lukas, J., Marcote, M. J., Pagano, M. & Draetta, G. 1993. Cyclin D1 is a nuclear protein required for cell cycle progression in G1. *Genes Dev,* 7**,** 812-21.

Barry, E. R., Morikawa, T., Butler, B. L., Shrestha, K., de la Rosa, R., Yan, K. S., Fuchs, C. S., Magness, S. T., Smits, R., Ogino, S., Kuo, C. J. & Camargo, F. D. 2013. Restriction of intestinal stem cell expansion and the regenerative response by YAP. *Nature,* 493**,** 106-10.

Brewer, J. R., Mazot, P. & Soriano, P. 2016. Genetic insights into the mechanisms of Fgf signaling. *Genes Dev,* 30**,** 751-71.

Cai, J., Cho, S. W., Kim, J. Y., Lee, M. J., Cha, Y. G. & Jung, H. S. 2007. Patterning the size and number of tooth and its cusps. *Dev Biol,* 304**,** 499-507.

Cam, Y., Neumann, M. R., Oliver, L., Raulais, D., Janet, T. & Ruch, J. V. 1992. Immunolocalization of acidic and basic fibroblast growth factors during mouse odontogenesis. *Int J Dev Biol,* 36**,** 381-9.

Castellano, E. & Downward, J. 2011. RAS Interaction with PI3K: More Than Just Another Effector Pathway. *Genes Cancer,* 2**,** 261-74.

Chambard, J. C., Lefloch, R., Pouyssegur, J. & Lenormand, P. 2007. ERK implication in cell cycle regulation. *Biochim Biophys Acta,* 1773**,** 1299-310.

Danielian, P. S., Muccino, D., Rowitch, D. H., Michael, S. K. & McMahon, A. P. 1998. Modification of gene activity in mouse embryos in utero by a tamoxifen-inducible form of Cre recombinase. *Curr Biol,* 8**,** 1323-6.

Dong, J., Feldmann, G., Huang, J., Wu, S., Zhang, N., Comerford, S. A., Gayyed, M. F., Anders, R. A., Maitra, A. & Pan, D. 2007. Elucidation of a universal size-control mechanism in Drosophila and mammals. *Cell,* 130**,** 1120-33.

Dong, X., Shen, B., Ruan, N., Guan, Z., Zhang, Y., Chen, Y. & Hu, X. 2014. Expression patterns of genes critical for BMP signaling pathway in developing human primary tooth germs. *Histochem Cell Biol,* 142**,** 657-65.

Edelman, G. M. 1992. Morphoregulation. *Dev Dyn,* 193**,** 2-10.

Elledge, S. J. 1996. Cell cycle checkpoints: preventing an identity crisis. *Science,* 274**,** 1664-72.

Gartel, A. L. & Radhakrishnan, S. K. 2005. Lost in transcription: p21 repression, mechanisms, and consequences. *Cancer Res,* 65**,** 3980-5.

Gokhale, R. H. & Shingleton, A. W. 2015. Size control: the developmental physiology of body and organ size regulation. *Wiley Interdiscip Rev Dev Biol,* 4**,** 335-56.

Heallen, T., Zhang, M., Wang, J., Bonilla-Claudio, M., Klysik, E., Johnson, R. L. & Martin, J. F. 2011. Hippo pathway inhibits Wnt signaling to restrain cardiomyocyte proliferation and heart size. *Science,* 332**,** 458-61.

Hu, X., Lee, J. W., Zheng, X., Zhang, J., Lin, X., Song, Y., Wang, B., Hu, X., Chang, H. H., Chen, Y., Lin, C. P. & Zhang, Y. 2018. Efficient induction of functional ameloblasts from human keratinocyte stem cells. *Stem Cell Res Ther,* 9**,** 126.

Hu, X., Lin, C., Shen, B., Ruan, N., Guan, Z., Chen, Y. & Zhang, Y. 2014a. Conserved odontogenic potential in embryonic dental tissues. *J Dent Res,* 93**,** 490-5.

636 Hu, X., Xu, S., Lin, C., Zhang, L., Chen, Y. & Zhang, Y. 2014b. Precise chronology of differentiation
637 of developing human primary dentition. *Histochem Cell Biol,* 141**,** 221-7.
638 Hu, X., Zhang, S., Chen, G., Lin, C., Huang, Z., Chen, Y. & Zhang, Y. 2013. Expression of SHH
639 signaling molecules in the developing human primary dentition. *BMC Dev Biol,* 13**,** 11.
640 Huang, F., Hu, X., Fang, C., Liu, H., Lin, C., Zhang, Y. & Hu, X. 2015. Expression profile of critical
641 genes involved in FGF signaling pathway in the developing human primary dentition.
642 *Histochem Cell Biol,* 144**,** 457-69.
643 Irazoqui, A. P., Boland, R. L. & Buitrago, C. G. 2014. Actions of 1,25(OH)2-vitamin D3 on the cellular
644 cycle depend on VDR and p38 MAPK in skeletal muscle cells. *J Mol Endocrinol,* 53**,** 331-
645 43.
646 Jernvall, J., Kettunen, P., Karavanova, I., Martin, L. B. & Thesleff, I. 1994. Evidence for the role of
647 the enamel knot as a control center in mammalian tooth cusp formation: non-dividing cells
648 express growth stimulating Fgf-4 gene. *Int J Dev Biol,* 38**,** 463-9.
649 Jernvall, J. & Thesleff, I. 2000. Reiterative signaling and patterning during mammalian tooth
650 morphogenesis. *Mech Dev,* 92**,** 19-29.
651 Jheon, A. H., Seidel, K., Biehs, B. & Klein, O. D. 2013. From molecules to mastication: the
652 development and evolution of teeth. *Wiley Interdiscip Rev Dev Biol,* 2**,** 165-82.
653 Jiang, T. X., Jung, H. S., Widelitz, R. B. & Chuong, C. M. 1999. Self-organization of periodic patterns
654 by dissociated feather mesenchymal cells and the regulation of size, number and spacing of
655 primordia. *Development,* 126**,** 4997-5009.
656 Kettunen, P. & Thesleff, I. 1998. Expression and function of FGFs-4, -8, and -9 suggest functional
657 redundancy and repetitive use as epithelial signals during tooth morphogenesis. *Dev Dyn,* 211**,**
658 256-68.
659 Kratochwil, K., Galceran, J., Tontsch, S., Roth, W. & Grosschedl, R. 2002. FGF4, a direct target of
660 LEF1 and Wnt signaling, can rescue the arrest of tooth organogenesis in Lef1(-/-) mice. *Genes*
661 *Dev,* 16**,** 3173-85.
662 Kurosaka, H., Islam, M. N., Kuremoto, K., Hayano, S., Nakamura, M., Kawanabe, N., Yanagita, T.,
663 Rice, D. P., Harada, H., Taniuchi, I. & Yamashiro, T. 2011. Core binding factor beta functions
664 in the maintenance of stem cells and orchestrates continuous proliferation and differentiation
665 in mouse incisors. *Stem Cells,* 29**,** 1792-803.
666 Kwon, H. J., Li, L. & Jung, H. S. 2015. Hippo pathway/Yap regulates primary enamel knot and dental
667 cusp patterning in tooth morphogenesis. *Cell Tissue Res,* 362**,** 447-51.
668 Lan, Y., Jia, S. & Jiang, R. 2014. Molecular patterning of the mammalian dentition. *Semin Cell Dev*
669 *Biol,* 25-26**,** 61-70.
670 Li, C. Y., Prochazka, J., Goodwin, A. F. & Klein, O. D. 2014. Fibroblast growth factor signaling in
671 mammalian tooth development. *Odontology,* 102**,** 1-13.
672 Lin, C., Yin, Y., Bell, S. M., Veith, G. M., Chen, H., Huh, S. H., Ornitz, D. M. & Ma, L. 2013.
673 Delineating a conserved genetic cassette promoting outgrowth of body appendages. *PLoS*
674 *Genet,* 9**,** e1003231.
675 Line, S. R. 2003. Variation of tooth number in mammalian dentition: connecting genetics,
676 development, and evolution. *Evol Dev,* 5**,** 295-304.
677 Liu, M., Zhao, S. & Wang, X. P. 2014. YAP overexpression affects tooth morphogenesis and enamel
678 knot patterning. *J Dent Res,* 93**,** 469-74.
679 Lloyd, A. C. 2013. The regulation of cell size. *Cell,* 154**,** 1194-205.

680 Lui, J. C., Garrison, P. & Baron, J. 2015. Regulation of body growth. *Curr Opin Pediatr,* 27**,** 502-10.
681 Matsuda, M., Hayashi, H., Garcia-Ojalvo, J., Yoshioka-Kobayashi, K., Kageyama, R., Yamanaka, Y.,
682 Ikeya, M., Toguchida, J., Alev, C. & Ebisuya, M. 2020. Species-specific segmentation clock
683 periods are due to differential biochemical reaction speeds. *Science,* 369**,** 1450-1455.
684 Michailovici, I., Harrington, H. A., Azogui, H. H., Yahalom-Ronen, Y., Plotnikov, A., Ching, S.,
685 Stumpf, M. P., Klein, O. D., Seger, R. & Tzahor, E. 2014. Nuclear to cytoplasmic shuttling of
686 ERK promotes differentiation of muscle stem/progenitor cells. *Development,* 141**,** 2611-20.
687 Morata, G. & Ripoll, P. 1975. Minutes: mutants of drosophila autonomously affecting cell division
688 rate. *Dev Biol,* 42**,** 211-21.
689 Penzo-Mendez, A. I. & Stanger, B. Z. 2015. Organ-Size Regulation in Mammals. *Cold Spring Harb*
690 *Perspect Biol,* 7**,** a019240.
691 Plikus, M. V., Zeichner-David, M., Mayer, J. A., Reyna, J., Bringas, P., Thewissen, J. G., Snead, M.
692 L., Chai, Y. & Chuong, C. M. 2005. Morphoregulation of teeth: modulating the number, size,
693 shape and differentiation by tuning Bmp activity. *Evol Dev,* 7**,** 440-57.
694 Polly, P. D. 2015. Gene networks, occlusal clocks, and functional patches: new understanding of
695 pattern and process in the evolution of the dentition. *Odontology,* 103**,** 117-25.
696 Promislow, D. E. L. & Harvey, P. H. 1990. Living fast and dying young: A comparative analysis of
697 life-history variation among mammals. *Proceedings of the Zoological Society of London,* 220**,**
698 417-437.
699 Rayon, T., Stamataki, D., Perez-Carrasco, R., Garcia-Perez, L., Barrington, C., Melchionda, M.,
700 Exelby, K., Lazaro, J., Tybulewicz, V. L. J., Fisher, E. M. C. & Briscoe, J. 2020. Species-
701 specific pace of development is associated with differences in protein stability. *Science,* 369.
702 Rodrigues, H. G., Renaud, S., Charles, C., Le Poul, Y., Sole, F., Aguilar, J. P., Michaux, J., Tafforeau,
703 P., Headon, D., Jernvall, J. & Viriot, L. 2013. Roles of dental development and adaptation in
704 rodent evolution. *Nat Commun,* 4**,** 2504.
705 Saebøe-Larssen, S., Lyamouri, M., Merriam, J., Oksvold, M. P. & Lambertsson, A. 1998. Ribosomal
706 protein insufficiency and the minute syndrome in Drosophila: a dose-response relationship.
707 *Genetics,* 148**,** 1215-24.
708 Salazar-Ciudad, I. 2012. Tooth patterning and evolution. *Curr Opin Genet Dev,* 22**,** 585-92.
709 Schoenwolf GC, B. S., Brauer PR, Francis-West PH 2014. Larsen's Human Embryology E-Book.
710 Song, H., Mak, K. K., Topol, L., Yun, K., Hu, J., Garrett, L., Chen, Y., Park, O., Chang, J., Simpson,
711 R. M., Wang, C. Y., Gao, B., Jiang, J. & Yang, Y. 2010. Mammalian Mst1 and Mst2 kinases
712 play essential roles in organ size control and tumor suppression. *Proc Natl Acad Sci U S A,*
713 107**,** 1431-6.
714 Song, Y., Zhang, Z., Yu, X., Yan, M., Zhang, X., Gu, S., Stuart, T., Liu, C., Reiser, J., Zhang, Y. &
715 Chen, Y. 2006. Application of lentivirus-mediated RNAi in studying gene function in
716 mammalian tooth development. *Dev Dyn,* 235**,** 1334-44.
717 Sonnen, K. F., Lauschke, V. M., Uraji, J., Falk, H. J., Petersen, Y., Funk, M. C., Beaupeux, M., François,
718 P., Merten, C. A. & Aulehla, A. 2018. Modulation of Phase Shift between Wnt and Notch
719 Signaling Oscillations Controls Mesoderm Segmentation. *Cell,* 172**,** 1079-1090 e12.
720 St Amand, T. R., Zhang, Y., Semina, E. V., Zhao, X., Hu, Y., Nguyen, L., Murray, J. C. & Chen, Y.
721 2000. Antagonistic signals between BMP4 and FGF8 define the expression of Pitx1 and Pitx2
722 in mouse tooth-forming anlage. *Dev Biol,* 217**,** 323-32.
723 Stockl, S., Bauer, R. J., Bosserhoff, A. K., Gottl, C., Grifka, J. & Grassel, S. 2013. Sox9 modulates

cell survival and adipogenic differentiation of multipotent adult rat mesenchymal stem cells. *J Cell Sci,* 126**,** 2890-902.

Swanson, E. M. & Dantzer, B. 2014. Insulin-like growth factor-1 is associated with life-history variation across Mammalia. *Proc Biol Sci,* 281**,** 20132458.

Tapaltsyan, V., Charles, C., Hu, J., Mindell, D., Ahituv, N., Wilson, G. M., Black, B. L., Viriot, L. & Klein, O. D. 2016. Identification of novel Fgf enhancers and their role in dental evolution. *Evol Dev,* 18**,** 31-40.

Thesleff, I. & Mikkola, M. 2002. The role of growth factors in tooth development. *Int Rev Cytol,* 217**,** 93-135.

Thesleff, I. & Sharpe, P. 1997. Signalling networks regulating dental development. *Mech Dev,* 67**,** 111-23.

Tucker, A. & Sharpe, P. 2004. The cutting-edge of mammalian development; how the embryo makes teeth. *Nat Rev Genet,* 5**,** 499-508.

Tumaneng, K., Russell, R. C. & Guan, K. L. 2012. Organ size control by Hippo and TOR pathways. *Curr Biol,* 22**,** R368-79.

Tummers, M. & Thesleff, I. 2009. The importance of signal pathway modulation in all aspects of tooth development. *J Exp Zool B Mol Dev Evol,* 312B**,** 309-19.

Vandomme, J., Touil, Y., Ostyn, P., Olejnik, C., Flamenco, P., El Machhour, R., Segard, P., Masselot, B., Bailliez, Y., Formstecher, P. & Polakowska, R. 2014. Insulin-like growth factor 1 receptor and p38 mitogen-activated protein kinase signals inversely regulate signal transducer and activator of transcription 3 activity to control human dental pulp stem cell quiescence, propagation, and differentiation. *Stem Cells Dev,* 23**,** 839-51.

Wang, B., Li, L., Du, S., Liu, C., Lin, X., Chen, Y. & Zhang, Y. 2010. Induction of human keratinocytes into enamel-secreting ameloblasts. *Dev. Biol.,* 344**,** 795-9.

Xiong, W., He, F., Morikawa, Y., Yu, X., Zhang, Z., Lan, Y., Jiang, R., Cserjesi, P. & Chen, Y. 2009. Hand2 is required in the epithelium for palatogenesis in mice. *Dev Biol,* 330**,** 131-41.

Xue, X. J. & Yuan, X. B. 2010. Nestin is essential for mitogen-stimulated proliferation of neural progenitor cells. *Mol Cell Neurosci,* 45**,** 26-36.

Yang, G., Yuan, G., Ye, W., Cho, K. W. & Chen, Y. 2014. An atypical canonical bone morphogenetic protein (BMP) signaling pathway regulates Msh homeobox 1 (Msx1) expression during odontogenesis. *J Biol Chem,* 289**,** 31492-502.

Yu, F. X., Zhao, B. & Guan, K. L. 2015. Hippo Pathway in Organ Size Control, Tissue Homeostasis, and Cancer. *Cell,* 163**,** 811-28.

Zaina, S. & Squire, S. 1998. The soluble type 2 insulin-like growth factor (IGF-II) receptor reduces organ size by IGF-II-mediated and IGF-II-independent mechanisms. *J Biol Chem,* 273**,** 28610-6.

Zhang, P., Pei, C., Wang, X., Xiang, J., Sun, B. F., Cheng, Y., Qi, X., Marchetti, M., Xu, J. W., Sun, Y. P., Edgar, B. A. & Yuan, Z. 2017. A Balance of Yki/Sd Activator and E2F1/Sd Repressor Complexes Controls Cell Survival and Affects Organ Size. *Dev Cell,* 43**,** 603-617 e5.

Zhang, Y., Wang, S., Song, Y., Han, J., Chai, Y. & Chen, Y. 2003. Timing of odontogenic neural crest cell migration and tooth-forming capability in mice. *Dev Dyn,* 226**,** 713-8.

Zhang, Y. D., Chen, Z., Song, Y. Q., Liu, C. & Chen, Y. P. 2005. Making a tooth: growth factors, transcription factors, and stem cells. *Cell Res,* 15**,** 301-16.

767 # Tables

768 **Table. 1 Ratio of tooth formation in different types of tissue recombinants.**

Type of Recombinant		No. of Recombinant	No. of Tooth Formation	Ratio (%)
Epithelium	Mesenchyme			
mde	mdm	28	28	100
mde	hdm	78	76	97.4
hde	mdm	27	24	88.9

769 Abbreviations: mdm, E13.5 mouse dental mesenchyme; hdm, bell-stage human dental mesenchyme
770 (14-16 weeks of gestation); mde, E13.5 mouse dental epithelium; hde, bell-stage human dental
771 epithelium (14-16 weeks of gestation).

772 # Figure legends

773 **Fig. 1. Heterogenous recombination of human and mouse embryonic dental tissues**
774 **reveals the dominant role of the dental mesenchyme in the control of tooth**
775 **developmental pace and size. A-C**: Azan dichromic staining (stains dentin blue and
776 enamel red) of recombinants of E13.5 mouse dental epithelium and bell-stage human
777 dental mesenchyme cultured under the kidney capsule for 3 weeks (**A**), 4 weeks (**B**), 8
778 weeks (**C**). Note that no deposition of dentin and enamel was seen in the chimeric tooth
779 germs until 4 weeks in subrenal culture. **D**: A lateral view of mde+hdm chimeric tooth
780 crowns after 16 weeks in subrenal culture. **E-G**: Azan dichromic staining of recombinants
781 of E13.5 mouse dental epithelium and E13.5 mouse dental mesenchyme cultured under
782 the kidney capsule for 6 days (**E**), 7 days (**F**), and 8 days (**G**). Note that the deposition of
783 dentin and enamel was not seen until 7 and 8 days, respectively, in subrenal culture. **H**:
784 A lateral view of mde+mdm tooth crowns after 30 days in subrenal culture. **I-K**: Azan
785 dichromic staining of recombinants of bell-stage human dental epithelium and E13.5
786 mouse dental mesenchyme cultured under the kidney capsule for 7 days (**I**), 9 days (**J**),
787 and 10 days (**K**). Note that the deposition of dentin and enamel was not seen until 9 and
788 10 days, respectively, in subrenal culture. **L**: A lateral view of hde+mdm chimeric tooth
789 crowns after 30 weeks in subrenal culture. **M-U**: The expression of ameloblastin and
790 MMP20 in recombinants of E13.5 mouse dental epithelium and bell-stage human dental
791 mesenchyme cultured under the kidney capsule for 3 weeks (**M**), 4 weeks (**N** and **O**), in
792 recombinants of E13.5 mouse dental epithelium and mouse dental mesenchyme for 6 days
793 (**P**), 7 days (**Q** and **R**), and in recombinants of bell-stage human dental epithelium and
794 mouse dental mesenchyme for 7 days (**S**) and 9 days (**T** and **U**). hdm, human dental
795 mesenchyme; hde, human dental epithelium; mdm, mouse dental mesenchyme; mde,
796 mouse dental epithelium; hod, human odontoblasts; mod, mouse odontoblasts; mam,
797 mouse ameloblasts; d, dentin; e, enamel. Scale bar: A-C, E-G, I-K, and M-U = 50 μm, D,
798 H, and L = 500 μm.

799

800 **Fig. 2. FGF signaling is involved in the regulation of tooth developmental pace and**
801 **size. A-C**: Immunostaining showing the expression of pSmad1/5/8 (**A**), K-Ras (**B**), and
802 β-catenin (**C**) in recombinants of mouse dental epithelium and mouse dental mesenchyme
803 cultured under the kidney capsule for 7 days. **D-F**: Immunostaining showing the
804 expression of pSmad1/5/8 (**D**), K-Ras (**E**), and β-catenin (**F**) in recombinants of mouse
805 dental epithelium and human dental mesenchyme cultured under the kidney capsule for
806 4 weeks. **G-H**: Human 1st premolar germs of 16th week gestation were transplanted under
807 the kidney capsule and cultured in the absence (**G**) or presence (**H**) of SU5402 for 1 week.
808 Note the accelerated detinogenesis with the appearance of dentin (**H**, red arrow) in the
809 presence of SU5402. **I-K**: Immunohistochemical staining showing the expression of
810 FGF4 (**I**), FGF8 (**J**), and FGF9 (**K**) in recombinants of mouse dental epithelium and
811 human dental mesenchyme cultured under the kidney capsule for 4 weeks. mam, mouse
812 ameloblasts; mod, mouse odontoblasts; hod, human odontoblasts; am, ameloblasts; od,
813 odontoblasts; sr, stellate reticulum; d, dentin; pre-d, predentin. Scale bar = 25 μm.
814
815 **Fig. 3. Augmented FGF8 signaling in the mouse dental mesenchyme delays tooth**
816 **development and increases cell proliferation. A**, **B**: Azan dichromic staining of
817 recombinants of E13.5 mouse dental epithelium and re-aggregate of dental mesenchymal
818 cells infected with control LV-*eGFP* (**A**) or LV-*Fgf8-eGFP* (**B**) cultured under the kidney
819 capsule for 6 days (insert in **A**), 7 days, and 9 days (insert in **B**). **C**, **D**: Immunostaining
820 showing the expression of Ki67 in recombinants of E13.5 mouse dental epithelium and
821 re-aggregate of dental mesenchymal cells infected with control LV-*eGFP* (**C**) or LV-*Fgf8-*
822 *eGFP* (**D**) cultured under the kidney capsule for 7 days. **E**: Comparison of Ki67-positive
823 cells in the dental mesenchyme and dental epithelium of the recombinants. Standard
824 deviation values were shown as error bars, and ** indicates $p<0.01$, $n = 6$/group. **F**: GFP
825 staining of recombinants of E13.5 mouse dental epithelium and re-aggregate of dental
826 mesenchymal cells infected with control LV-*eGFP* cultured under the kidney capsule for
827 11 days. dm, dental mesenchyme; dp, dental pulp; am, ameloblasts; sr, stellate reticulum;
828 od, odontoblasts; d, dentin; Epi, epithelium; Mes, mesenchyme. Scale bar = 50 μm.
829

830 **Fig. 4. Delayed tooth development in early molar germs of *Wnt1-Cre;R26R^{Fgf8}* mice.**
831 **A-H:** H&E staining showing the morphology of maxillary and mandibular molar in E13.5
832 wild-type (**A**,**C**) and mutant (**B**,**D**) embryos and in E14.5 wild-type (**E**,**G**) and mutant
833 (**F**,**H**) embryos. de, dental epithelium; dm, dental mesenchyme. Scale bar = 50 μm.
834
835 **Fig. 5. Grafts of *Wnt1-Cre;R26R^{Fgf8}* molar germs exhibit delayed tooth development**
836 **and enlarged tooth size. A-H**: Azan dichromic staining of E11.5 wild-type and mutant
837 molar germs cultured under the kidney capsule for 8 days (**A**,**B**), 9 days (**C**,**D**), 10 days
838 (**E**,**F**), and 18 days (**G**,**H**). **I-L**: Immunostaining showing the expression of DSP (**I,J**) and
839 Ameloblastin (**K,L**) in E11.5 wild-type and mutant molar grafts cultured under the kidney
840 capsule for 9 days. **M**, **N**: Representative Micro-CT images of E11.5 wild-type (**M**) and
841 mutant molar germs (**N**) cultured under the kidney capsule for 3 months. **O**: Comparison
842 of the height and width of the tooth crown between wild-type and mutant mineralized
843 teeth cultured under the kidney capsule for 3 months. Standard deviation values were
844 shown as error bars. ns indicates $p > 0.05$, and ** indicates $p < 0.01$, $n = 7$ and 11/group
845 in **O**. de, dental epithelium; dm, dental mesenchyme; am, ameloblasts; od, odontoblasts;
846 d, dentin; e, enamel. Scale bar: A-H, I-L = 50 μm; M and N = 500 μm.
847
848 **Fig. 6. Ectopically activated dental mesenchymal FGF8 signaling stimulates cell**
849 **proliferation and prevents cell apoptosis during odontogenesis. A-F**: Immunostaining
850 showing the Ki67 positive cells in E13.5 wild-type (**A**) and mutant (**D**) molar germs and
851 in the grafts of E11.5 wild-type and mutant molar germ cultured under the kidney
852 capsule for 9 days (**B**,**E**) and 18 days (**C**,**F**). **G-J**: Immunostaining showing the expression
853 of Caspase3 in the grafts of E11.5 wild-type (**G**, boxed area is magnified in **H**) and mutant
854 (**I**, boxed area is magnified in **J**) molar germ cultured under the kidney capsule for 18
855 days. Note the absence of Caspase3 expression in the dental mesenchyme (red asterisk)
856 excepting odontoblasts in mutant grafts. **K-M**: The percentage of Ki67 positive cells in
857 the dental mesenchyme of wild-type and mutant E13.5 tooth germs (**K**) and tooth grafts
858 cultured under the kidney capsule for 9 days (**I**) and 18 days (**M**), $n = 3$/group, * indicates
859 $p < 0.05$. Standard deviation values were shown as error bars. am, ameloblasts; od,

860 odontoblasts; d, dentin; e, enamel. Scale bar = 100 μm.

861

862 **Fig. 7. Ectopically activated dental mesenchymal FGF8 signaling is transduced via**
863 **p38 and PI3K-Akt intracellular pathways. A-D**: Immunostaining showing the
864 expression of pErk1/2 in E13.5 wild-type (**A**) and mutant (**B**) molar germs and in E11.5
865 wild-type (**C**) and mutant (**D**) molar germs cultured under the kidney capsule for 9 days.
866 **E-H**: Immunostaining showing the expression of pJNK in E13.5 wild-types (**E**) and
867 mutants (**F**) molar germs and in E11.5 wild-type (**G**) and mutant (**H**) molar germs cultured
868 under the kidney capsule for 9 days. **I-L**: Immunostaining showing the expression of pP38
869 in E13.5 wild-type (**I**) and mutant (**J**) molar germs and in E11.5 wild-type (**K**) and mutant
870 (**L**) cultured under the kidney capsule for 9 days. **M-P**: Immunostaining showing the
871 expression of pAkt1 in E13.5 wild-types (**M**) and mutants (**N**) molar germs and in E11.5
872 wild-type (**O**) and mutant (**P**) molar germs cultured under the kidney capsule for 9 days.
873 **Q**: Western-blotting of pErk1/2, pP38, pJNK, and pAKT1 expressed in E13.5 wild-type
874 and mutant molar germs. **R**: Quantification of immunoblotting data in **Q**. n = 3/group. *
875 indicates $p < 0.05$. Standard deviation values were shown as error bars. de, dental
876 epithelium; dm, dental mesenchyme; am, ameloblasts; od, odontoblasts. Scale bar = 25
877 μm.

878

879 **Fig. 8. Enhanced dental mesenchymal FGF8 signaling increases the level of nuclear**
880 **Ccnd1 and decreases the level of nuclear p21.** Immunostaining showing the
881 colocalization of Ccnd1 and P21 in E13.5 wild-type (**A-D**) and mutant (**E-H**) molar germs
882 and E11.5 wild-type (**I-L**) and mutant (**M-P**) molar germs cultured under the kidney
883 capsule for 9 days. Boxed areas in (**C**), (**G**), (**K**), and (**O**) are magnified in (**D**), (**H**), (**L**),
884 and (**P**), respectively. Note the significantly increased proportion of Ccnd1-positive cells
885 (white arrow) and the shift of P21 from the nuclei to the cytoplasm (yellow arrow) in the
886 mutant dental mesenchyme (**P**) as compared with wild-type ones (**L**). de, dental
887 epithelium; dm, dental mesenchyme; am, ameloblasts; od, odontoblasts. Scale bar: A-N,
888 P-S = 50 μm; O, T = 25 μm.

889

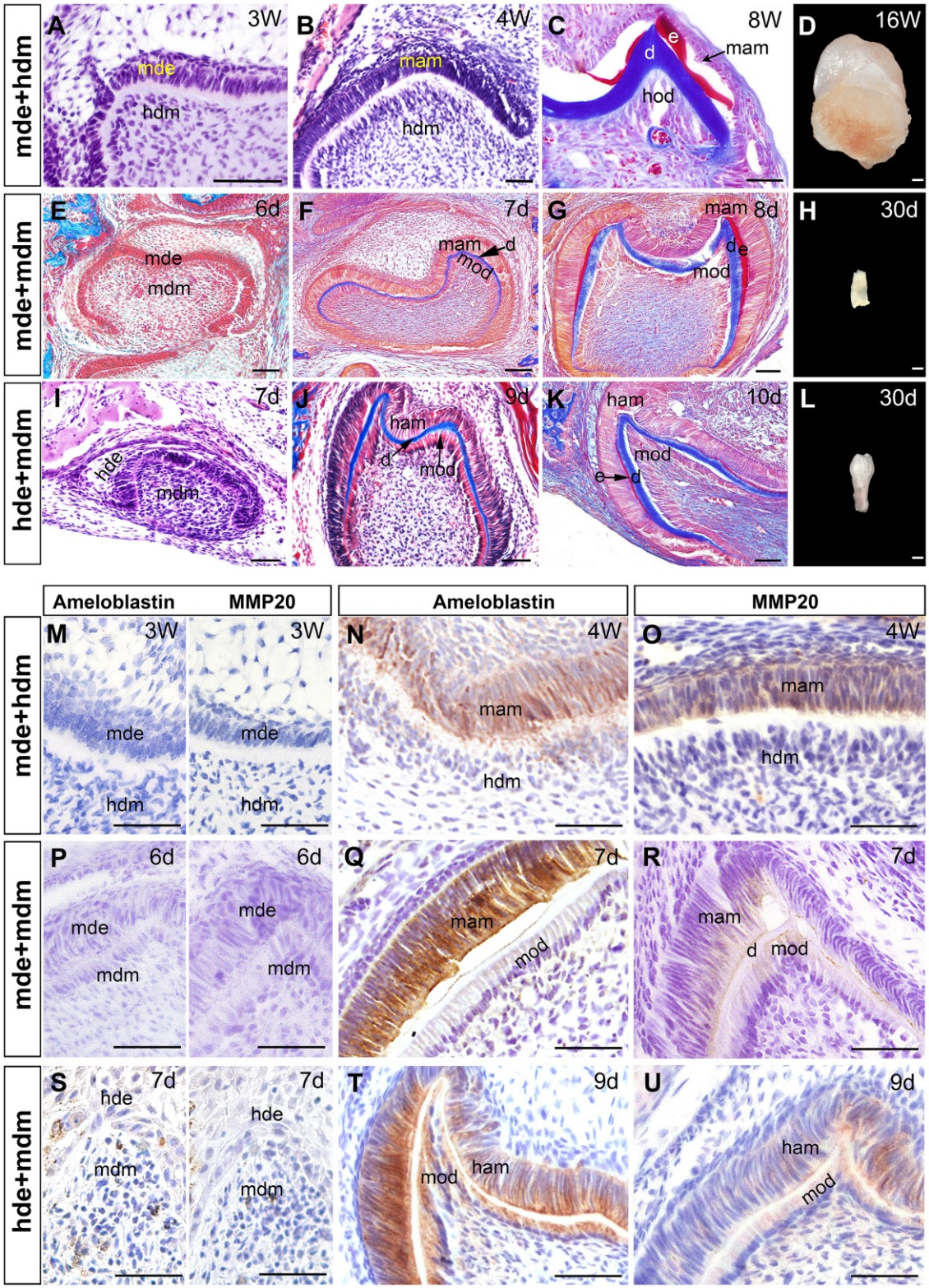
mde+hdm
mde+mdm
hde+mdm
A 3W
mde
hdm
B 4W
mam
hdm
C 8W
e
d
mam
hod
D 16W
E 6d
mde
mdm
F 7d
mam
d
mod
G 8d
mam
de
mod
H 30d
I 7d
hde
mdm
J 9d
ham
d
mod
K 10d
ham
mod
e
d
L 30d
Ameloblastin
MMP20
Ameloblastin
MMP20
M 3W
mde
hdm
3W
mde
hdm
N 4W
mam
hdm
O 4W
mam
hdm
P 6d
mde
mdm
6d
mde
mdm
Q 7d
mam
mod
R 7d
mam
d
mod
S 7d
hde
mdm
7d
hde
mdm
T 9d
mod
ham
U 9d
ham
mod

Figure 1

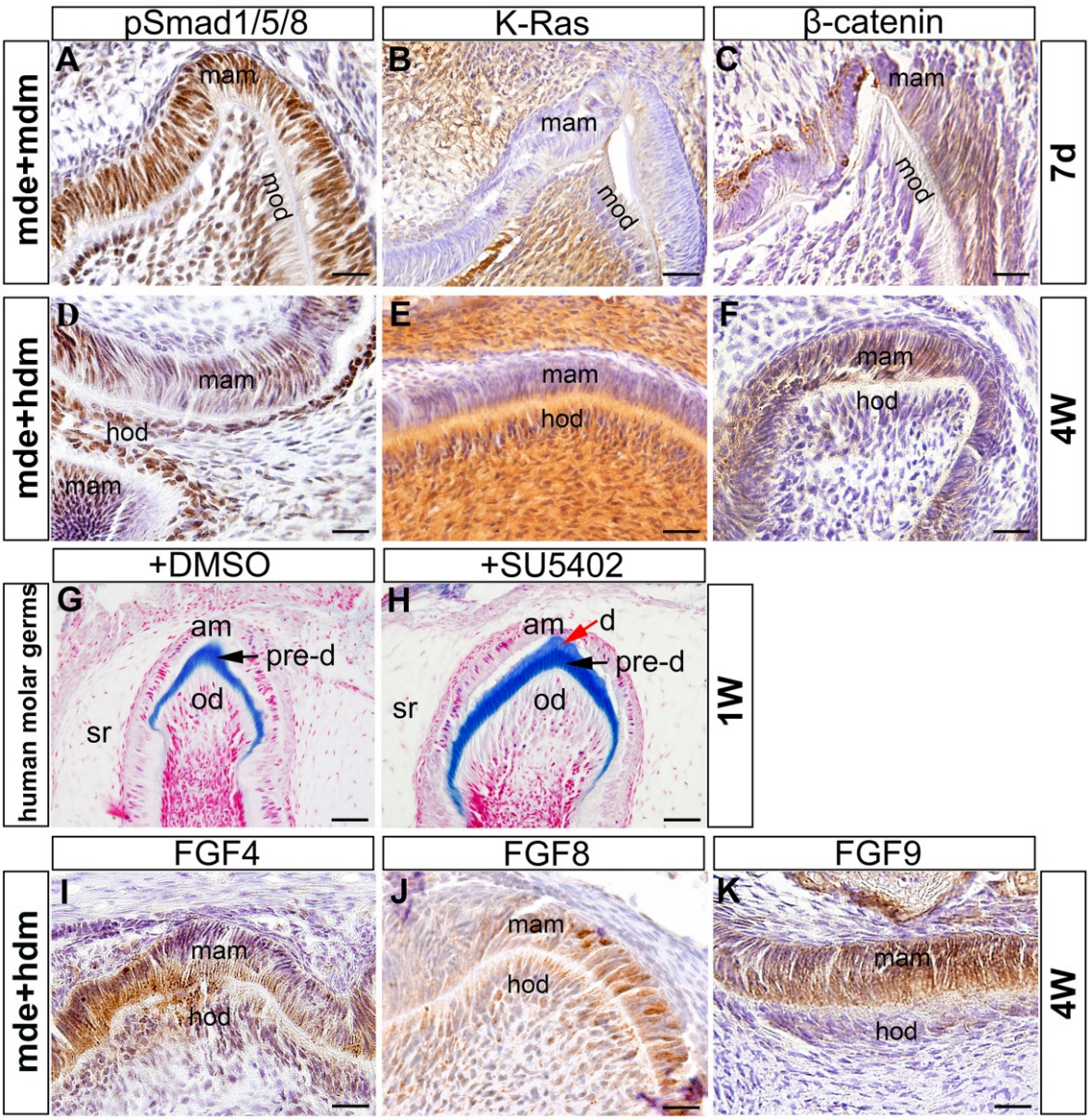
pSmad1/5/8
K-Ras
β-catenin
mde+mdm
7d
A
mam
mod
B
mam
mod
C
mam
mod
mde+hdm
4W
D
mam
hod
mam
E
mam
hod
F
mam
hod
+DMSO
+SU5402
human molar germs
1W
G
am
pre-d
od
sr
H
am
d
pre-d
od
sr
FGF4
FGF8
FGF9
mde+hdm
4W
I
mam
hod
J
mam
hod
K
mam
hod

Figure 2

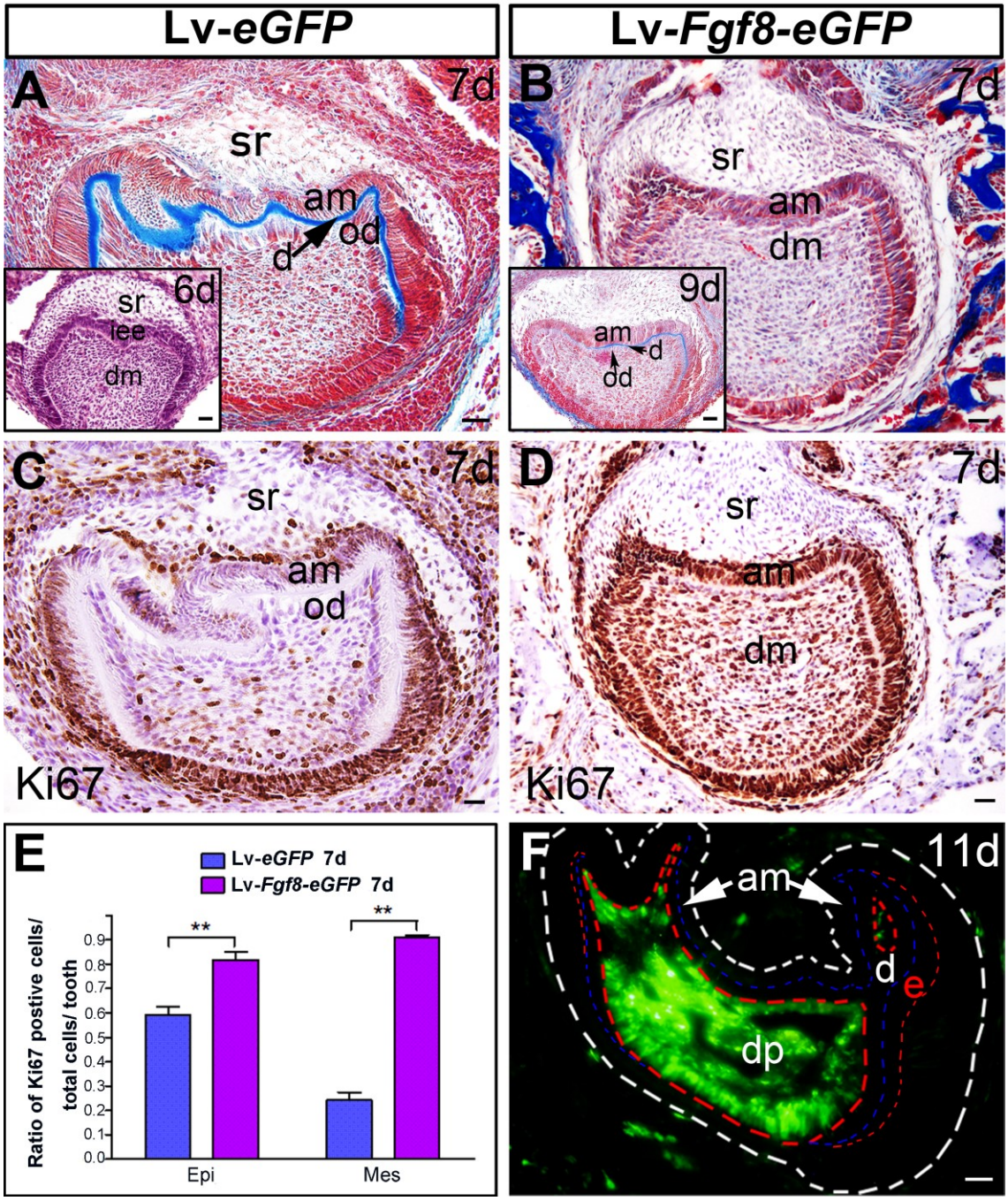
Lv-eGFP
Lv-Fgf8-eGFP
A
7d
sr
am
od
d
6d
sr
iee
dm
B
7d
sr
am
dm
9d
am
d
od
C
7d
sr
am
od
Ki67
D
7d
sr
am
dm
Ki67
E
Lv-eGFP 7d
Lv-Fgf8-eGFP 7d
Ratio of Ki67 postive cells/ total cells/ tooth
0.0
0.1
0.2
0.3
0.4
0.5
0.6
0.7
0.8
0.9
**
**
Epi
Mes
F
11d
am
d
e
dp

Figure 3

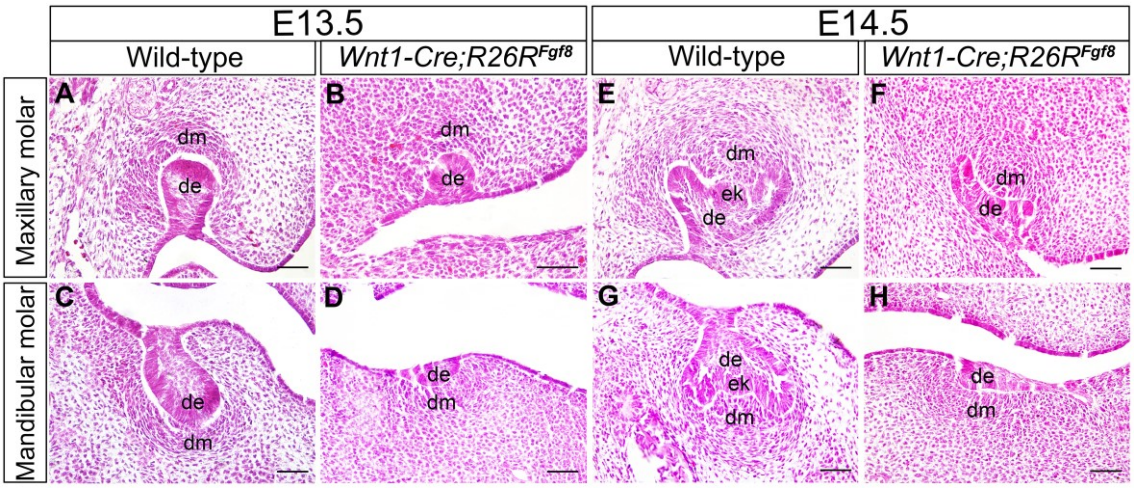

Figure 4

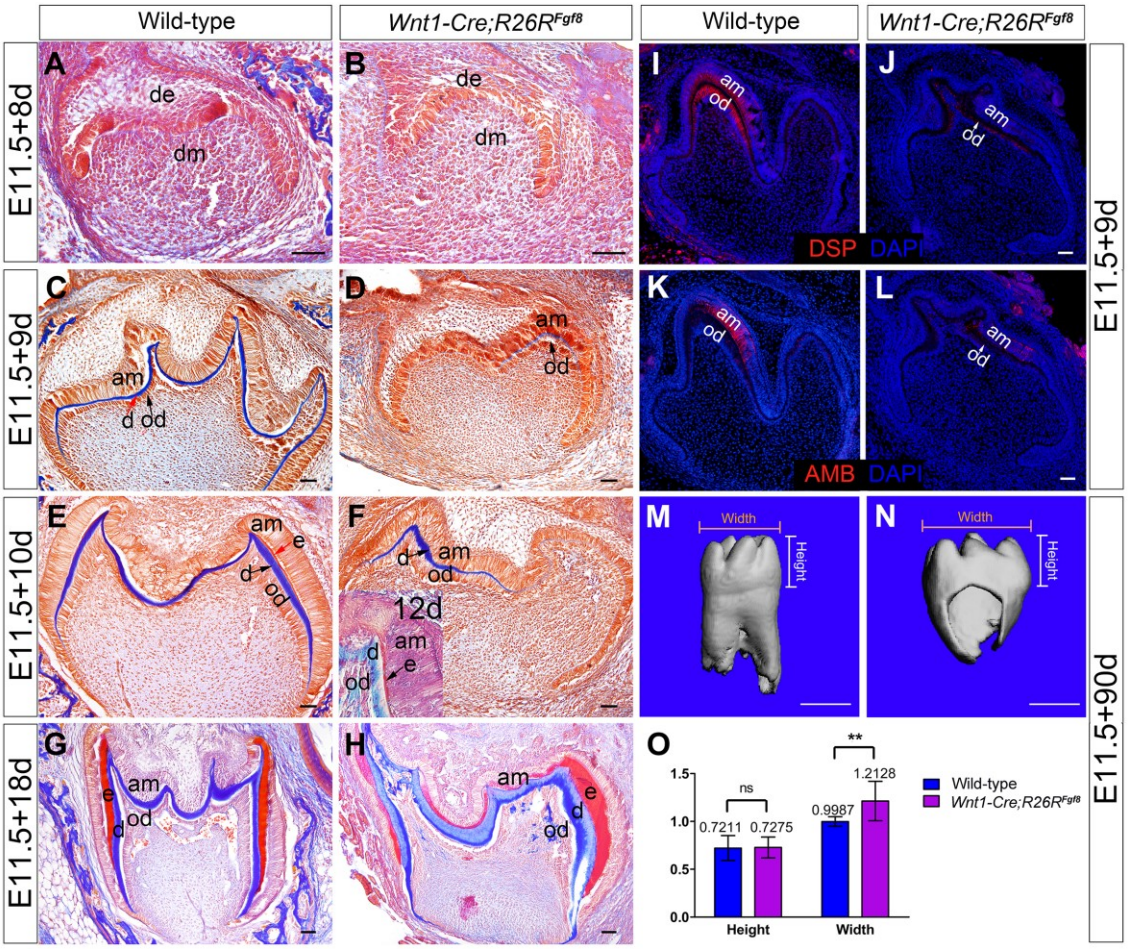

Figure 5

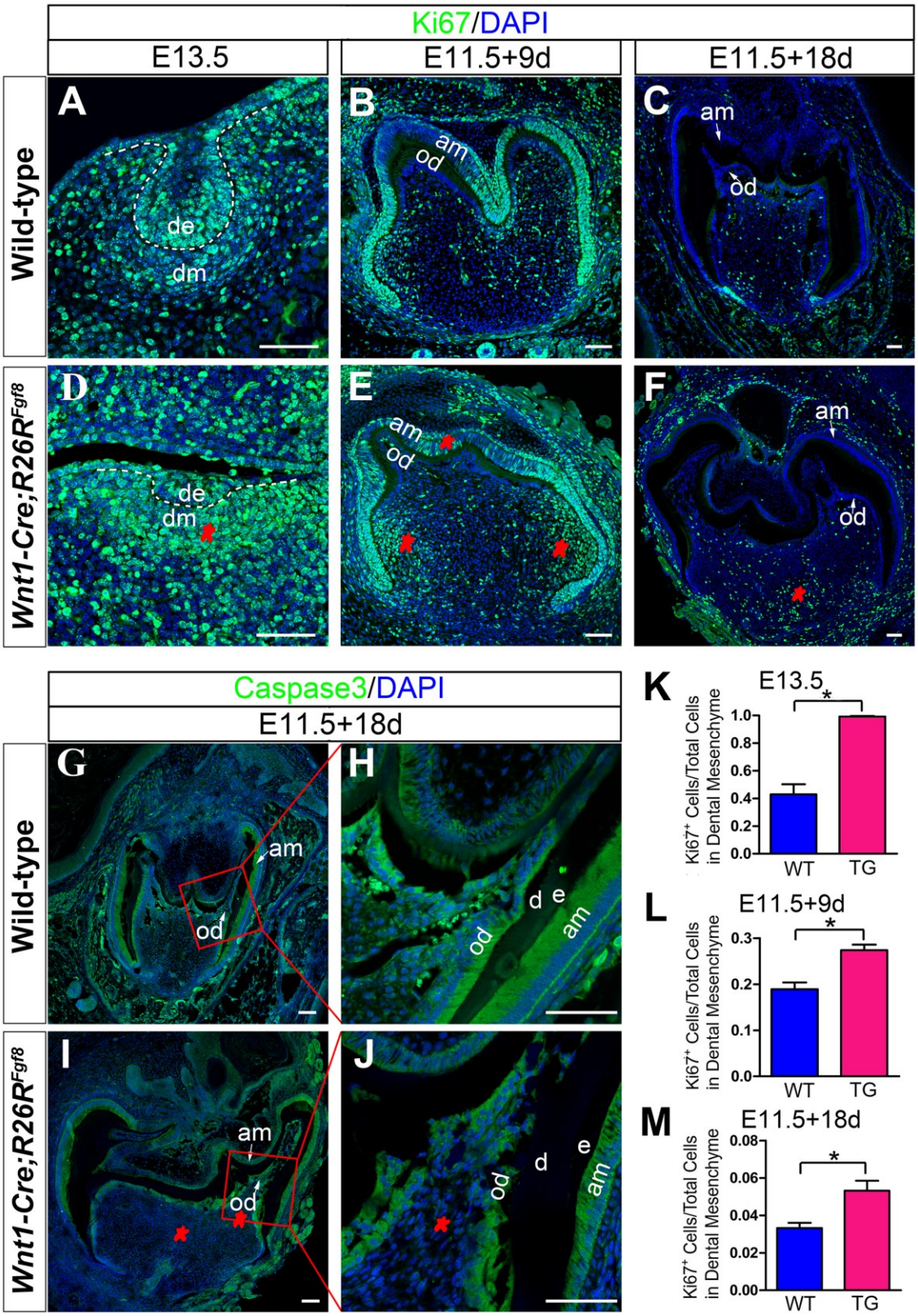
Ki67/DAPI
E13.5
E11.5+9d
E11.5+18d
Wild-type
Wnt1-Cre;R26R^Fgf8
A
B
C
D
E
F
de
dm
am
od
Caspase3/DAPI
E11.5+18d
G
H
I
J
d
e
K
L
M
E13.5
E11.5+9d
E11.5+18d
Ki67+ Cells/Total Cells in Dental Mesenchyme
WT
TG
*

Figure 6

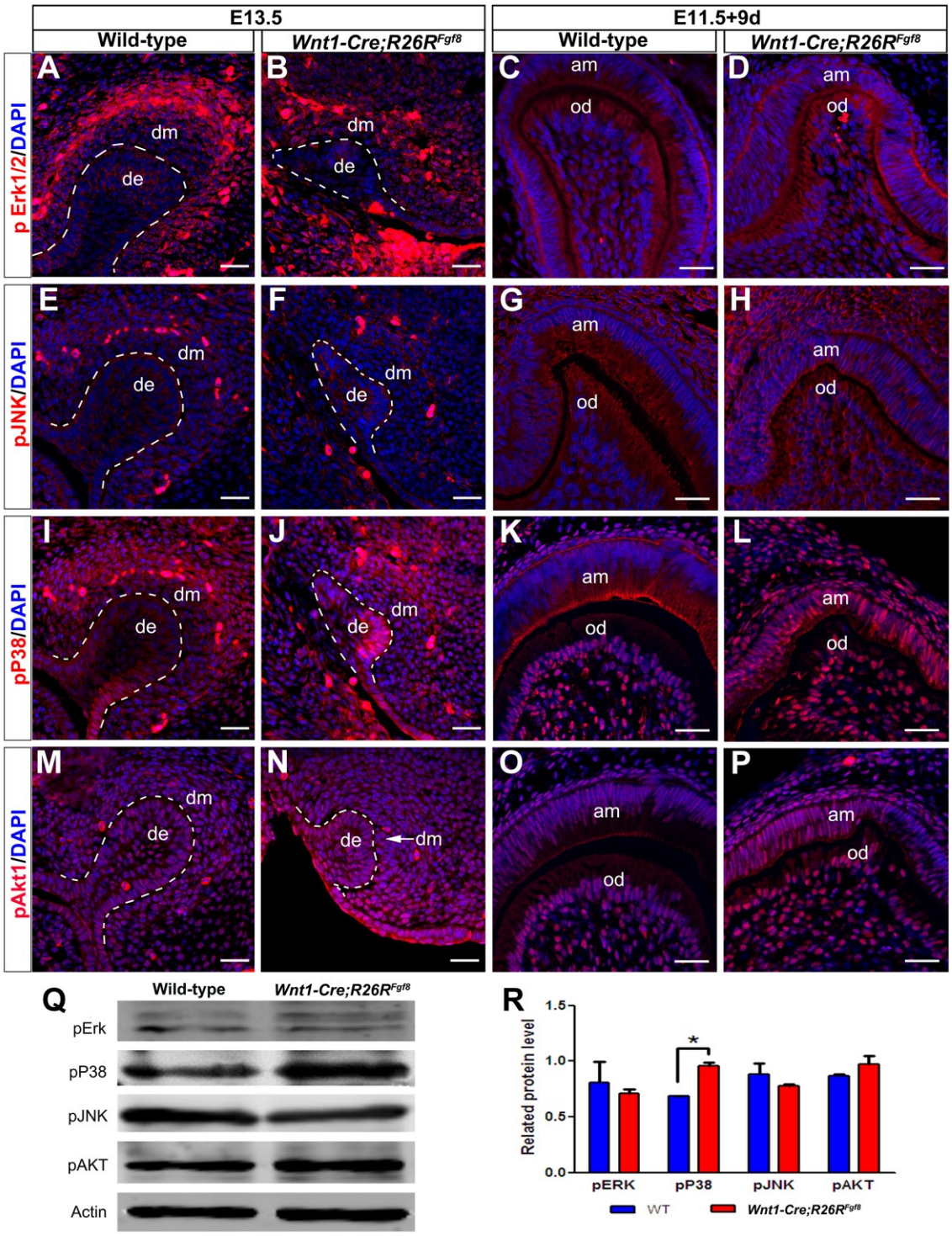
E13.5
E11.5+9d
Wild-type
Wnt1-Cre;R26R^Fgf8
p Erk1/2/DAPI
pJNK/DAPI
pP38/DAPI
pAkt1/DAPI
dm
de
am
od
Q
pErk
pP38
pJNK
pAKT
Actin
R
Related protein level
1.5
1.0
0.5
0.0
*
pERK
pP38
pJNK
pAKT
WT
Wnt1-Cre;R26R^Fgf8

Figure 7

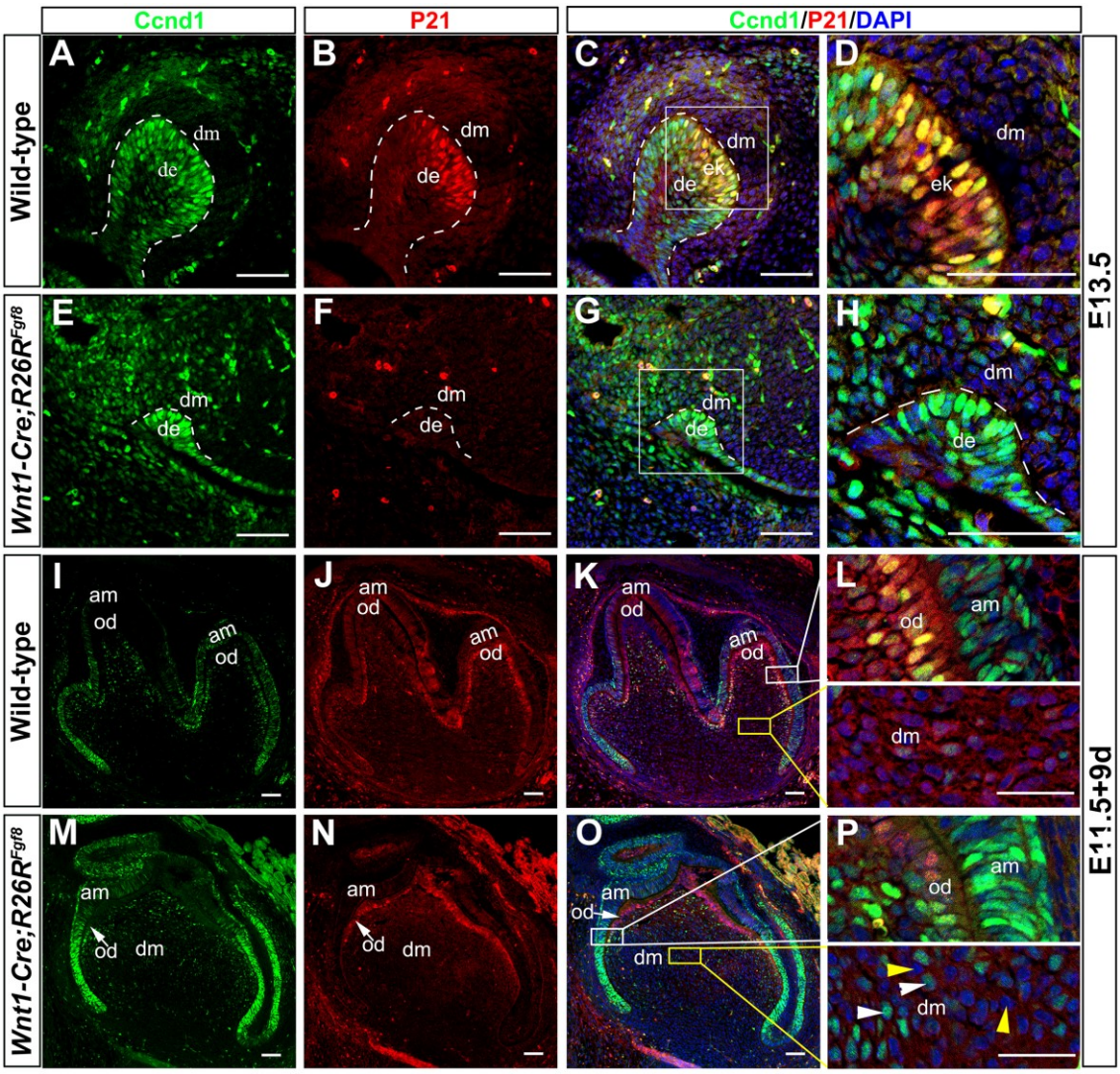
Ccnd1
P21
Ccnd1/P21/DAPI
Wild-type
Wnt1-Cre;R26R^Fgf8
E13.5
E11.5+9d
A
B
C
D
E
F
G
H
I
J
K
L
M
N
O
P
dm
de
ek
am
od

Figure 8